

1 **Remote Sensing for Drought Monitoring & Impact Assessment: Progress, Past**
2 **Challenges and Future Opportunities**

3

4 **Harry West, Nevil Quinn & Michael Horswell**

5 Centre for Water, Communities & Resilience; Department of Geography & Environmental
6 Management; University of the West of England, Bristol

7

8 Corresponding Author: Harry West (harry.west@uwe.ac.uk)

9

10

11

12

13

14

15

16

17

18

19

20

21

22

23

24 **Remote Sensing for Drought Monitoring & Impact Assessment: Progress, Past**
25 **Challenges and Future Opportunities**

26

27 **Abstract**

28 Drought is a common hydrometeorological phenomenon and a pervasive global hazard. As
29 our climate changes, it is likely that drought events will become more intense and frequent.
30 Effective drought monitoring is therefore critical, both to the research community in
31 developing an understanding of drought, and to those responsible for drought management
32 and mitigation. Over the past 50 years remote sensing has shifted the field away from
33 reliance on traditional site-based measurements and enabled observations and estimates of
34 key drought-related variables over larger spatial and temporal scales than was previously
35 possible. This has proven especially important in data poor regions with limited in-situ
36 monitoring stations. Available remotely sensed data products now represent almost all
37 aspects of drought propagation and have contributed to our understanding of the
38 phenomena. In this review we chart the rise of remote sensing for drought monitoring,
39 examining key milestones and technologies for assessing meteorological, agricultural and
40 hydrological drought events. We reflect on challenges the research community has faced to
41 date, such as limitations associated with data record length and spatial, temporal and
42 spectral resolution. This review then looks ahead to the future in terms of new technologies,
43 such as the ESA Sentinel satellites, analytical platforms and approaches, such as Google
44 EarthEngine, and the utility of existing data in new drought monitoring applications. We
45 look forward to the continuation of 50 years of progress to provide effective, innovative and
46 efficient drought monitoring solutions utilising remote sensing technology.

47

48 **Keywords**

49 Drought; Drought Monitoring; Meteorological Drought; Agricultural Drought; Hydrological
50 Drought; Remote Sensing of Drought; Review Paper.

51

52 **1.0 Introduction**

53 Drought is a common hydrometeorological phenomenon (Hayes *et al.*, 2012), and a
54 pervasive hazard, second only to flooding in its impact on social and economic security
55 (Nagarajan, 2009). Since the turn of the century, several socio-economically significant
56 regional droughts have occurred, for example in Australia (2000-2009), USA (2000-2016),
57 Southern and Sub-Saharan Africa (2015-2017), China (2007-2012) and Europe (2007-2010)
58 (Ummenhofer *et al.*, 2009; Ault *et al.*, 2016; Chao *et al.*, 2016; Cook *et al.*, 2016; Baudoin *et*
59 *al.*, 2017). There is no universal definition of a drought (Lloyd-Hughes, 2014), but in its
60 simplest form a drought event represents a deficit of water relative to normal conditions.
61 Unlike floods which have a clear and sudden start and end (Wang *et al.*, 2016), droughts can
62 be characterised by slow development and prolonged impacts. How spatio-temporally
63 variable rainfall deficits propagate through the land surface to register deficits in soil
64 moisture, runoff and recharge is complex and heterogeneous. While droughts can be ended
65 by sudden extreme precipitation, how to precisely identify the termination point of a
66 drought event is contested (Parry *et al.*, 2016). These attributes mean that drought is a
67 phenomenon that is challenging to quantify and analyse. Impacts from recent droughts
68 reveal high levels of exposure and vulnerability of both natural and human systems (Van
69 Loon *et al.*, 2016). This is significant as with future climate change it is likely that many areas
70 will start to experience more frequent and intense dry conditions, with irreversible impacts

71 for people and ecosystems (IPCC, 2014). Consequently, drought monitoring and mitigation
72 have become urgent scientific issues (Liu *et al.*, 2016).

73

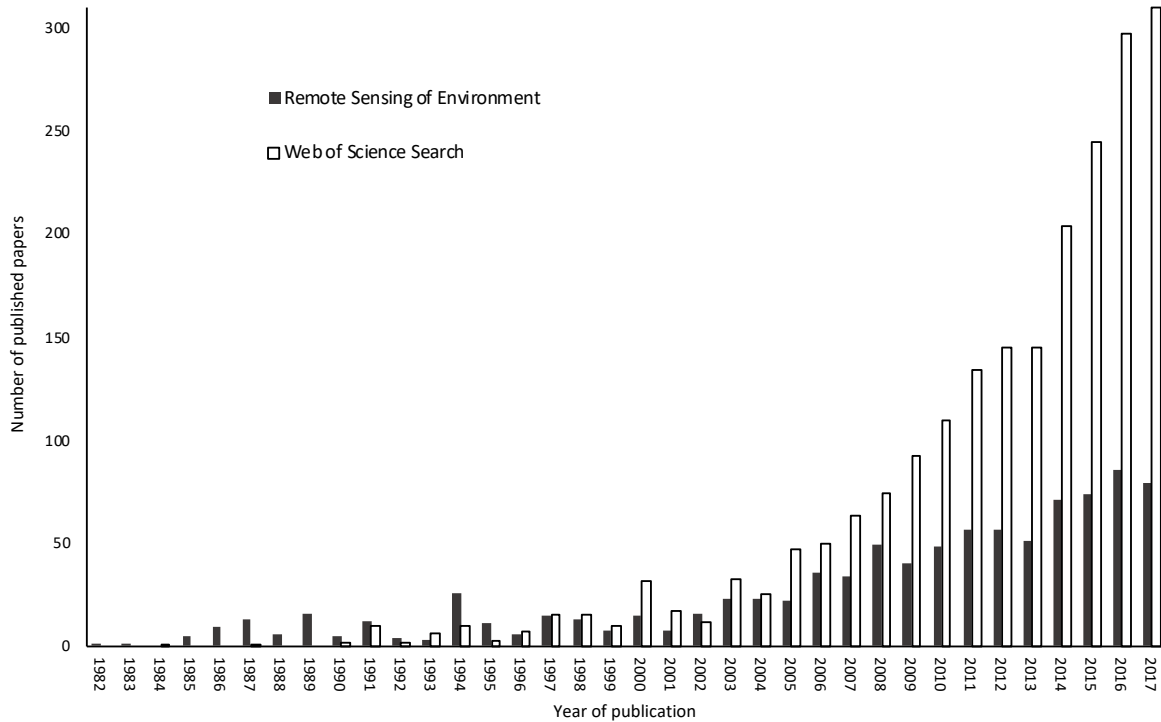
74 Historically drought monitoring approaches have focused on in-situ station-based
75 measurements, for example the Palmer Drought Severity Index (PDSI) (Palmer, 1965).

76 Towards the end of the 20th century a paradigm shift in drought monitoring approaches
77 occurred, concurrent with advances in remote sensing and earth observation technologies
78 such as the launch of the NASA Landsat series in 1972. In addition to providing
79 meteorological data, remote sensing-based approaches also monitor conditions at the
80 Earth's surface such as vegetation health and water levels, providing a rich mix of contextual
81 data for drought monitoring. Remote sensing has consequently revolutionised the field,
82 allowing observations and monitoring of key drought-related variables over larger temporal
83 and spatial scales than was previously possible using conventional methods (Choi *et al.*,
84 2013; Sur *et al.*, 2015). The role of remote sensing technologies for effective water
85 management has been highlighted as of particular importance in developing 'data-poor
86 regions' (Sheffield *et al.*, 2018).

87

88 This paradigm shift in drought monitoring approaches is marked in the number of drought-
89 related papers appearing in *Remote Sensing of Environment*; from less than 5 per year in
90 1982, to more than 70 per year since 2014 (Figure 1). Other journals (e.g. *Remote Sensing*,
91 *International Journal of Applied Earth Observation and Geoinformation* and *International*
92 *Journal of Remote Sensing*), have also seen a significant increase, and this is the case in
93 hydrology and water management research journals too (Lettenmaier *et al.*, 2015).

94

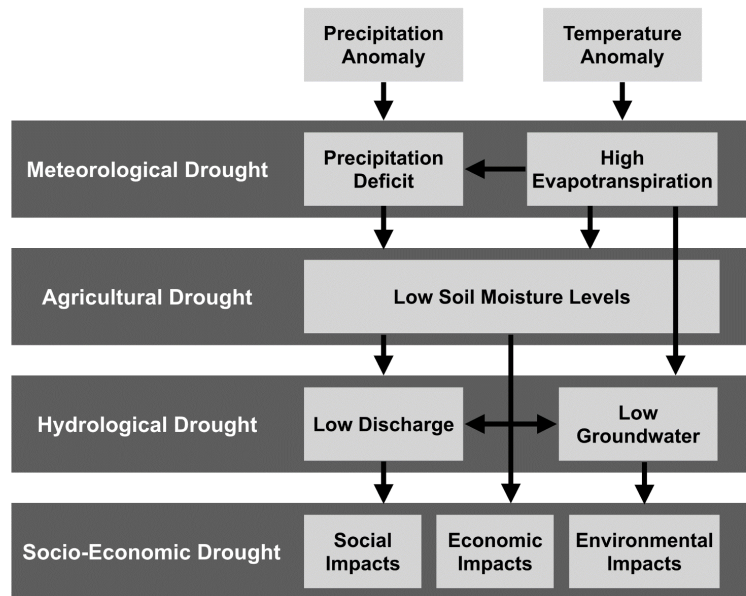


95

96 **Figure 1:** Number of papers relating to drought (in both paper titles and keywords) in
 97 *Remote Sensing of Environment* and *Web of Science* since 1982. Search terms included
 98 various versions of ‘Drought’ and ‘Remote Sensing’.

99

100 Although droughts are complex phenomena which propagate in different ways with varied
 101 characteristics, they are commonly classified into one of four types, namely meteorological
 102 drought, agricultural drought, and hydrological drought (which represent the
 103 natural/environmental impacts), and socio-economic drought (which represents the impact
 104 on human population and society) (Van Loon, 2015; Liu *et al.*, 2016). These types are not
 105 independent but refer to different approaches of measurement and identification (Wilhite
 106 & Glantz, 1985) (Figure 2).



107

108 **Figure 2:** Different types of drought, their interactions and associated impacts (Adapted
 109 from Van Loon, 2015)

110

111 Drought propagation is the process whereby a precipitation deficit (i.e. below average
 112 rainfall) progresses through the hydrological cycle, starting with meteorological drought and
 113 developing into hydrological drought if conditions persist (Van Loon, 2015). Factors
 114 influencing the nature of drought propagation include regional climate and local catchment
 115 characteristics, such as geology, vegetation cover and type, soils, topography and human
 116 influence (Van Loon & Laaha, 2015; Baker *et al.*, 2016). Given the complex characteristics of
 117 drought, event heterogeneity, and various propagation pathways and influences, remote
 118 sensing can provide a valuable tool in the monitoring of a range of drought-related
 119 variables.

120

121 This review will focus on the remote sensing-based monitoring of ‘environmental drought’,
 122 that is events that can be classified as being either meteorological, agricultural or
 123 hydrological drought and the relationships between them. Since the start of remote sensing

124 application in the field of drought monitoring active and passive sensors, recording
125 measurements across the electromagnetic spectrum, have been used to improve
126 understanding and inform environmental management decisions. Recent years have seen
127 rapid evolution in remote sensing technologies which can be applied in drought monitoring,
128 such as the launch of the ESA Sentinel satellites and the development of new indicators and
129 analytical platforms. Given the rate of technological evolution it is important to
130 continuously review and reflect upon historic and recent developments and look ahead to
131 new opportunities.

132

133 **2.0 Precipitation Monitoring**

134 Meteorological drought typically results from the presence of continuously high
135 atmospheric pressure over a region, representing a significant negative deviation from
136 mean precipitation (Sheffield & Wood, 2011). Meteorological droughts tend to occur over
137 relatively short time scales, usually days/weeks but possibly extending into months/seasons
138 (Pal *et al.*, 2000), and the associated precipitation deficit is the propagation trigger for
139 agricultural and hydrological drought. Unlike the other drought types, a meteorological
140 drought will typically have few direct impacts (Sen, 2015). Nonetheless, given
141 meteorological drought is often an early indicator of more impactful and significant dry
142 events, effective monitoring is still critical.

143

144 Historically, site-based precipitation measurements were essential for meteorological
145 drought monitoring, but the introduction of remote sensing precipitation products changed
146 the efficiency and spatio-temporal coverage of rainfall mapping and drought monitoring
147 (e.g. Islam & Uyeda, 2005; Islam & Uyda, 2007; Almazroui, 2011; Du *et al.*, 2013; Zhang *et*

148 *al.*, 2017a). The first of these was the TRMM (Tropical Rainfall Measuring Mission), a joint
149 collaboration between NASA and the Japan Aerospace Exploration Agency (JAXA). Launched
150 in 1997 and decommissioned in 2015, TRMM measured tropical and subtropical rainfall
151 (35°S - 35°N) and was the first satellite to carry a specific microwave precipitation radar
152 (Kummerow *et al.*, 1998). Due to its restricted orbital cycle TRMM completed 16 cycles per
153 day, with a measurement swath of 878km and spatial resolution of 0.25 degrees at the time
154 of decommissioning. The 17-year legacy dataset represents a significant benchmark in
155 global rainfall measurement and is still routinely used in assessing global rainfall patterns
156 and atmospheric drivers of drought (e.g. Zhang & Jia, 2013; Sahoo *et al.*, 2015; Forootan *et*
157 *al.*, 2016; Yan *et al.*, 2018). The successor to TRMM is the Global Precipitation Measurement
158 (GPM) mission (Hou *et al.*, 2014). The GPM Core Observatory was launched in February
159 2014. This also operates in a non-polar, low inclination orbit completing 16 cycles per day,
160 however with a wider coverage than TRMM (65°S - 65°N). Along with a constellation of
161 other satellites this gives a revisit time for GPM products of 1-2 hours, with an improved
162 spatial resolution (0.1-0.25 degrees). Studies have assessed the accuracy of GPM retrievals
163 at various scales through correlation with in-situ gauged data and TRMM data (Tang *et al.*,
164 2016; Libertino *et al.*, 2016; Caracciolo *et al.*, 2018), with results suggesting high levels of
165 agreement. Consequently, GPM and coupled TRMM/GPM datasets have become important
166 products in drought monitoring research (e.g. Zhang *et al.*, 2017b; Alizadeh & Nikoo, 2018).
167
168 Studies have used a range of analytical approaches when employing remotely sensed
169 precipitation in drought monitoring, including the calculation of long-term rainfall anomalies
170 (e.g. Toté *et al.*, 2015; Bayissa *et al.*, 2017; Cattani *et al.*, 2018) and indices, such as the
171 Precipitation Condition Index (PCI) (Zhang *et al.*, 2017a). One of the most commonly used

172 indices that can be derived from remote sensing data is the Standardised Precipitation Index
173 (SPI). Developed by McKee *et al.* (1993), the SPI is calculated using precipitation alone,
174 which meant at the time it was far more data efficient than the PDSI for many applications.
175 The main advantage of the SPI is that the values have the same probability of occurrence,
176 no matter the time period, location, or scale, and equally represent both flood/wet and
177 drought/dry events along a continuum. Until recently, its use has been limited in remote
178 sensing studies, due to the need for a long-term precipitation record for calculation
179 (traditionally ~30 years). However, with long-term records now becoming available it is
180 possible to calculate SPI using remotely sensed data alone, enabling detection of
181 meteorological droughts over large spatial scales (e.g. Sahoo *et al.*, 2015; Winkler *et al.*,
182 2017; Elhang & Zhang, 2018; Zhao *et al.*, 2018).

183

184 **3.0 Evapotranspiration Monitoring**

185 As discussed above, the onset of meteorological drought is often a key predictor of
186 agricultural/hydrological drought. Consequently, it is common for research to attempt to
187 integrate meteorological drought-related variables into studies which aim to assess and
188 improve the monitoring of these other drought types. A key factor of both meteorological
189 and agricultural drought is the increase in evapotranspiration rates (Figure 2). Reliable
190 estimation of evapotranspiration is essential for effective drought monitoring and the
191 development of hydrologic models (Fisher *et al.*, 2017). As with precipitation, a key benefit
192 of using remotely sensed products is the ability to assess evaporation/evapotranspiration
193 over large areas, and in the absence of in-situ monitoring stations. Calculation of
194 evaporation/evapotranspiration requires additional variables relating to vegetation
195 condition and type and/or soil properties (Narasimhan & Srinivasan, 2005) and these can be

196 estimated through remote sensing. As such, various evapotranspiration remote sensing data
197 products now exist - derived from observations from a range of satellite families, such as the
198 MODIS and Landsat satellites.

199

200 The Global Land Evaporation Amsterdam Model (GLEAM) (Miralles *et al.*, 2011) is a set of
201 algorithms for estimating terrestrial evaporation and soil moisture. The approach was
202 revised in 2014 (Miralles *et al.*, 2014) and is currently on its third iteration (Martens *et al.*,
203 2017). The current GLEAM product consists of a series of microwave (C- and L-band)
204 measurements of vegetation, soil moisture and precipitation and thermal observations of
205 land surface temperature (LST), from sensors such as MODIS (Moderate Resolution Imaging
206 Spectroradiometer) and the SMOS (Soil Moisture Ocean Salinity) mission (Martens *et al.*,
207 2017). The uniqueness of GLEAM is that it is the only global scale evaporation product
208 designed to be driven by remotely sensed data alone (Miralles *et al.*, 2011). Given that
209 GLEAM uses data from sensors which have a long operational history, Version 3.3 of the
210 product is available for the period 1980-2018.

211

212 Many drought-related studies using remotely sensed precipitation or evapotranspiration
213 products have been at global or continental scales (Sahoo *et al.*, 2015; Xia *et al.*, 2018), and
214 necessarily at coarse spatial resolution (Huffman *et al.*, 1997; Martens *et al.*, 2017). This may
215 be because many of the earlier earth observation satellites prioritised temporal over spatial
216 resolution (Lettenmaier *et al.*, 2015). However, attempts have recently been made to
217 increase the spatial resolution of meteorological remotely sensed data. For example, van
218 Dijk *et al.* (2018) used MODIS observations of surface water extent, vegetation, and LST,
219 assimilated into a landscape hydrological model, to derive a 5km resolution global scale

220 dataset of secondary evaporation (i.e. evaporation from floodplain/wetland storage and
221 irrigation systems).

222

223 Passive sensor derived datasets have also been re-analysed to represent
224 evaporation/evapotranspiration. For example, the Landsat satellites have been used in the
225 development of new, higher resolution, monitoring approaches (Wulder *et al.*, 2019). With
226 the addition of the thermal band on Landsat 3 (launched in 1978), which was later enhanced
227 on Landsat 4 (1982) onwards, high resolution (30m visible and 120m thermal) retrievals of
228 land classifications and LST were made possible. These observations have led to the retrieval
229 of relatively high-resolution estimates of evapotranspiration (Vinukollu *et al.*, 2011). Recent
230 work has been undertaken using the Google EarthEngine (Gorelick *et al.*, 2017) to calculate
231 key meteorological/hydrological variables using the thermal capabilities of space-borne
232 sensors. EEFlux (EarthEngine Evapotranspiration Flux) was developed based on the METRIC
233 (Mapping Evapotranspiration at High Resolution with Internalized Calibration) model (Allen
234 *et al.*, 2007) and applies a series of algorithms to produce evapotranspiration estimates
235 using Landsat 5 TM (1984-2013), Landsat 7 ETM+ (1999-Present) and Landsat 8 OLI-TIRS
236 (2013-Present) imagery.

237

238 **4.0 Vegetation & Soil Moisture Monitoring**

239 Sustained meteorological drought over a region will begin to impact upon local hydrology
240 and agriculture (Dutra *et al.*, 2014). Agricultural drought (also referred to as soil moisture
241 drought) represents a deficit in soil moisture available to vegetation driven by a
242 precipitation deficit (meteorological drought) (Liu *et al.*, 2016). Agricultural droughts tend to

243 occur over medium to long term time scales and associated impacts include crop yield
244 reductions or failure, and eventually food demand/supply disequilibrium.
245
246 Remotely sensed agricultural drought monitoring can be via measurement of soil moisture
247 content, usually through microwave radar (active) and radiometers (passive) such as SMOS
248 or SMAP (Soil Moisture Active Passive) (e.g. Martínez-Fernández *et al.*, 2016; Mishra *et al.*,
249 2017; Rajasekaran *et al.*, 2018), or through the assessment of vegetation using passive
250 multispectral sensors such as Landsat or more recently Sentinel-2/-3 (e.g. Gu *et al.*, 2008:
251 Zhang *et al.*, 2017a; Myoung-Jin *et al.*, 2018). The former represents a direct measurement
252 of soil moisture, while the latter infer this by assessing vegetation condition or productivity.

253

254 *4.1 Passive Multispectral Remote Sensing Approaches*

255 In the late 20th and early 21st century various multispectral indices, applicable in drought
256 monitoring, were developed. These include the Normalised Difference Vegetation Index
257 (NDVI) (Tucker, 1979), the Normalised Difference Water Index (NDWI) (Gao, 1996), the Soil
258 Adjusted Vegetation Index (SAVI) (Huete, 1988), and the Vegetation Condition Index (VCI)
259 (Kogan, 1995a) and the Temperature Condition Index (TCI) (Kogan, 1995b), which were later
260 combined into the Vegetation Health Index (VHI) (Kogan, 1997).

261

262 Of these, the most well-established approach to agricultural drought monitoring is the
263 NDVI. The NDVI's success derives from its exploitation of the 'red-edge' (the sharp increase
264 in vegetation reflectance across the red and near-infrared regions of the electro-magnetic
265 spectrum) to detect photosynthetically active plant material, from which plant stress can be
266 inferred as the available moisture within the root zone is depleted (Wang *et al.*, 2007; Chen

267 *et al.*, 2014; Ahmed *et al.*, 2017; West *et al.*, 2018). The NDVI is calculated using the near-
268 infrared (NIR) and visible red bands of a multispectral sensor (Equation 1).

269

$$270 \quad NDVI = \frac{NIR-RED}{NIR+RED} \quad (\text{Equation 1})$$

271

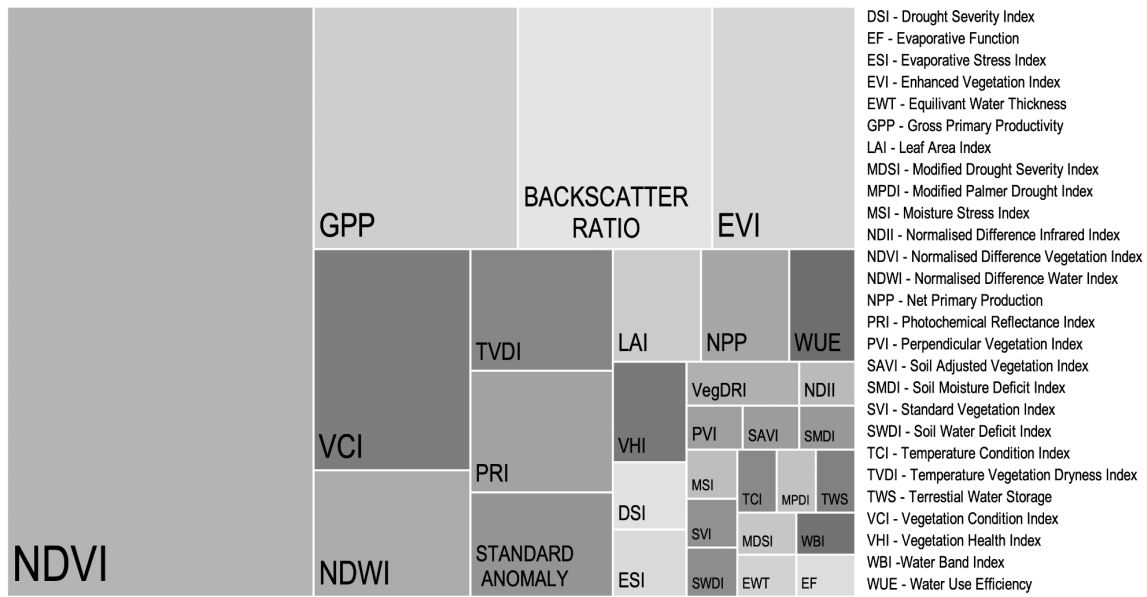
272 The logic for the use of the NDVI for agricultural drought monitoring is that soil moisture
273 plays a significant role in the sustained growth and healthiness of vegetation (Lavender &
274 Lavender, 2016). Should soil moisture drop below a certain threshold vegetation will
275 respond by wilting, lowering the NDVI due to a weakening of the leaf tissue structure and
276 reduced chlorophyll content.

277

278 One of the first applications of NDVI based drought monitoring used the NOAA (National
279 Oceanic & Atmospheric Administration) AVHRR (Advanced Very High-Resolution
280 Radiometer). Launched in 1979, AVHRR enabled global scale vegetation mapping with a
281 frequent revisit period (Tucker *et al.*, 1983). This was followed by numerous studies which
282 aimed to refine the AVHRR NDVI products by accounting for atmospheric conditions, cloud
283 masking, scale, temporal lags, amongst other variables (Holben & Fraser, 1984; Gatlin *et al.*,
284 1984; Townshend *et al.*, 1985; Holben, 1986; Loveland *et al.*, 1991; Gutman, 1991; Eastman
285 & Fulk, 1993; Stone *et al.*, 1994).

286

287 As of September 2018, the combined search of NDVI and drought using Scopus returns 983
288 scientific journal articles published since 1979. In a literature review of drought-related
289 papers, the NDVI is featured as a key index in more than 30% of the 300 agricultural drought
290 related papers reviewed (Figure 3).



293 **Figure 3:** Treemap of monitoring approaches used in agricultural drought monitoring of the
 294 papers reviewed. Papers were sourced from a range of journals including *Remote Sensing of*
 295 *Environment, Remote Sensing, and the International Journal of Remote Sensing.*

297 NDVI-based drought monitoring has been conducted using a broad range of sensors over
 298 global, continental, regional and catchment scales (e.g. Park *et al.*, 2004; Bayarjargal *et al.*,
 299 2006; Neigh *et al.*, 2008; Rojas *et al.*, 2011; Nicolai-Shaw *et al.*, 2017). Drought assessment
 300 and monitoring using NDVI has been undertaken across North America (e.g. Hwang *et al.*,
 301 2017), South America (e.g. Sayago *et al.*, 2017), Europe (e.g. Zribi *et al.*, 2016), the Middle
 302 East (e.g. Pervez *et al.*, 2014), Australia (e.g. Chen *et al.*, 2014), Asia (e.g. Yu *et al.*, 2003) and
 303 Africa (e.g. Funk & Brown, 2006). Few studies using these sensors have successfully
 304 attempted to assess vegetation at finer more local scales, in particular when vegetation is
 305 highly heterogeneous or sparse, due to sensor spatial/spectral resolution limitations (e.g.
 306 Assal *et al.*, 2016).

308 More recently, studies using hyper-spatial/-spectral imagery (captured using very high
309 spatial and spectral resolution satellites, aircraft, or ground-based/tram sensors) have also
310 applied the NDVI to examine agricultural drought. For example, the Quickbird and RapidEye
311 satellite sensors have shown great potential for high spatial resolution (~1m) assessment of
312 drought impacts on vegetation (Garrity *et al.*, 2013; Krofcheck *et al.*, 2014), with results
313 suggesting that vegetation dynamics closely reflect precipitation deficits at the field scale
314 (Laliberte *et al.*, 2004). The majority of this high-/hyper-resolution research has been based
315 in North America and Europe (e.g. Calaudio *et al.*, 2006; Mänd *et al.*, 2010; Coates *et al.*,
316 2015), most likely due to the expense of obtaining such imagery, or the instalment of
317 ground-based sensor systems, which cannot as easily be met in less developed regions.

318

319 NDVI based approaches do however have limitations. For example the NDVI only represents
320 conditions on one specific date and does not show condition relative to longer term change,
321 is easily influenced by soil brightness in areas of low-density vegetation (Huete, 1988;
322 Jasinski, 1990), and, at the other end of the spectrum, is limited in its sensitivity in high
323 density biomass environments (Mutanga *et al.*, 2012; Galidaki *et al.*, 2016). The Vegetation
324 Health Index (VHI) (Kogan, 1997) was seen to offer notable improvements over standalone
325 NDVI-based monitoring as it provides a representation of vegetation condition relative to
326 long term change. The VHI is a weighted average of two sub-indices: the VCI (Kogan, 1995a)
327 and the TCI (Kogan, 1995b)

328

329
$$VCI = \frac{(NDVI - NDVI_{min}) \times 100}{NDVI_{max} - NDVI_{min}} \text{ (Equation 2)}$$

330
$$TCI = \frac{100 (BT_{max} - BT)}{BT_{max} - BT_{min}} \text{ (Equation 3)}$$

331
$$VHI = \alpha \times VCI + (1 - \alpha) \times TCI \text{ (Equation 4)}$$

332

333 Where max/min represent the maximum and minimum values of that variable over the
334 study period and BT is Brightness Temperature recorded from a thermal sensor. The VCI
335 pixel-based normalisation minimises any spurious or short-term signals in the data and
336 amplifies the long-term trend (Anyamba & Tucker, 2012). Studies assessing the VCI have
337 found that both NDVI anomalies and the VCI are correlated with rainfall deficits, but the VCI
338 offers a more robust comparison of seasonal drought conditions (Liu & Kogan, 1996). The
339 VCI is commonly used, with results suggesting the index is effective in monitoring vegetation
340 change and agricultural drought at continental scales (Jiao *et al.*, 2016; Winkler *et al.*, 2017).

341

342 The TCI makes use of thermal remote sensing technologies and measurements of LST. LST
343 computed from thermal infrared bands, from sensors such as AVHRR and Landsat (Landsat 3
344 onwards), has been found to provide valuable information on surface moisture conditions
345 (Gutman, 1990). As a result, efforts have been made to merge multispectral vegetation
346 indices with measurements from thermal-equipped sensors, such as the Temperature
347 Vegetation Drought Index (TVDI) (Sandholt *et al.*, 2002) or the Vegetation Supply Water
348 Index (VSWI) (Haboudane *et al.*, 2004). Compared to NIR-based vegetation indices alone,
349 temperature/brightness indices have been found to be more sensitive to soil water stress
350 (Wang *et al.*, 2004).

351

352 By the time of its publication (1997) the VHI had successfully been used in research in parts
353 of Asia, Europe, North America and Africa (Kogan, 1994a; 1994b; 1995a; 1995b). The VHI
354 has been used in applications of drought management (e.g. San Miguel-Ayanz *et al.*, 2000;

355 Qu *et al.*, 2019), in the development of more complex remote sensing monitoring
356 approaches (e.g. Brown *et al.*, 2008), and in vegetation health and crop studies (e.g. Rahman
357 *et al.*, 2009). The VCI/VHI have also been used in combination with other indices such as the
358 NDWI and Enhanced Vegetation Index (EVI) (Huete *et al.*, 2002). The value of a multi-index
359 approach is that different indices have been found to have differing sensitivities to factors
360 including vegetation type/density/biomass and soil brightness (Prabhakara *et al.*, 2015).

361

362 Given the main socio-economic impact of agricultural drought is the potential disequilibrium
363 between the demand and supply of food/crops, being able to accurately monitor crop
364 growth and productivity is of particular importance. A commonly used method to assess
365 vegetation growth and productivity is to calculate gross primary productivity (GPP) (Figure
366 3). GPP represents the rate at which vegetation converts light into energy via
367 photosynthesis (Gilabert *et al.*, 2015). New sensors and analytical approaches have meant
368 that traditional hydrological methods of calculating GPP have been revisited (Rossini *et al.*,
369 2012). Many approaches now use satellite data in combination with models and other
370 datasets (Song *et al.*, 2013; Anav *et al.*, 2015; Joiner *et al.*, 2018). In the papers reviewed it
371 was common for GPP to be based on the light-use efficiency (LUE) method of Monteith
372 (1972) (Equation 5).

373

$$374 \quad \text{GPP} = \text{LUE} \times \text{FAPAR}_{\text{chl}} \times \text{PAR}_{\text{in}} \text{ (Equation 5)}$$

375

376 Where PAR_{in} is top of canopy photosynthetically-active radiation and $\text{FAPAR}_{\text{chl}}$ is the fraction
377 of PAR_{in} absorbed by chlorophyll. The inclusion of remotely sensed data has largely been to
378 provide a value for $\text{FAPAR}_{\text{chl}}$. The NDVI is one of the most commonly used proxies of

379 FAPAR_{chl} (e.g. Zhang *et al.*, 2009; Rossini *et al.*, 2012; Joiner *et al.*, 2018). Therefore, a
380 revision to Equation 5 would be:

381

$$382 \quad GPP = S \times VI \times PAR_{in} \text{ (Equation 6)}$$

383

384 Where VI is the selected vegetation index to represent FAPAR_{chl} and S is a constant
385 representing LUE (Sims *et al.*, 2008). A range of satellites and sensors have been used to
386 calculate the VI element of Equation 6 (Nightingale *et al.*, 2007; Zhang *et al.*, 2014; Dong *et al.*,
387 2015; Bayat *et al.*, 2018). This includes some hyper-resolution sensors (Krofcheck *et al.*,
388 2014; Gitelson *et al.*, 2018). Findings suggest that GPP is an important variable for
389 monitoring drought and is more sensitive to non-typical dry conditions than traditional VIs
390 such as the NDVI and EVI (Wagle *et al.*, 2014). Sims *et al.* (2008) also note the non-linear
391 relationship between GPP and LST under extreme drought conditions (compared to a linear
392 relationship under normal conditions). This is likely due to the low values and highly variable
393 nature of VIs under drought conditions (owing to poor quality/stressed vegetation or sparse
394 coverage). GPP has also proved useful in the detection of irrigated/non-irrigated fields in
395 droughty southern USA (Peng *et al.*, 2013; Doughty *et al.*, 2018).

396

397 Beyond calculation of GPP, some drought monitoring studies have further calculated the
398 Water Use Efficiency (WUE) of crops (e.g. Lu & Zhang, 2010; Ahmadi *et al.*, 2019). WUE is
399 defined as the ratio of leaf carbon uptake to water loss (Morison & Morecroft, 2006). WUE
400 can be calculated using Equation 7

401

$$402 \quad WUE = \frac{\text{Volume of water used productively}}{\text{Volume of water potentially available}} \text{ (Equation 7)}$$

403

404 The volume of water used productively is taken as GPP, and the volume of water available
405 as evapotranspiration (Huang *et al.*, 2015; Yang *et al.*, 2016). MODIS GPP and
406 evapotranspiration products have been used to calculate WUE with results showing similar
407 patterns to GPP under drought conditions. For example, Lu & Zhuang (2010) show non-
408 linear trends between WUE and drought intensity; with WUE increasing under moderate
409 conditions but decreasing sharply under severe drought.

410

411 While the development of multispectral and thermal indices from passive sensors has been
412 of interest to the research community for some time, Kogan (1997) noted that while
413 technology was advancing indices such as the NDVI and VHI, at the time, had not yet been
414 ground-truthed or validated against traditional monitoring techniques. To an extent this is
415 still true today, with issues around accuracy and uncertainty in remotely sensed data still a
416 challenge (Liu *et al.*, 2016). However, as demand has grown for continuous and reliable
417 data, studies have examined the relationship between traditional approaches/ground
418 measurements and remote sensing observations. Wang *et al.* (2007) found that MODIS
419 derived NDVI at 16km spatial resolution produced statistically significant correlations
420 between NDVI and measured soil moisture. Gu *et al.* (2008) conducted similar analysis also
421 using MODIS derived NDVI, finding that correlation between NDVI and measured soil
422 moisture was dependent on landcover heterogeneity and soil type. Areas with homogenous
423 vegetation cover and silt loams produced the highest correlations, while areas with
424 heterogenous vegetation cover and loam soils produced the lowest correlations. The
425 correlation between remote sensing and traditional meteorological/ground-based indices
426 and data is significant in the field of remote sensing-based drought monitoring. Remote

427 sensing indices offer a multi-scaled approach, and do not rely on site-based climatic
428 datasets which are sparse in many parts of the world (Choi *et al.*, 2013; Sur *et al.*, 2015). As
429 satellites are able to observe areas of the Earth where such ground-based datasets do not
430 exist, effective drought monitoring and management can still take place.

431

432 *4.2 Microwave Remote Sensing Approaches*

433 Both active and passive sensors which record measurements in the microwave segment of
434 the EMS have been applied in agricultural drought monitoring research. Active microwave
435 sensors (radar/scatterometers) use backscatter strength to determine moisture conditions.
436 Retrievals of soil moisture content from active microwave sensors can characterise key
437 drought variables, including the intensity, frequency and spatial extent of soil moisture
438 deficit. A key benefit of microwave sensors is they can provide continuous coverage over
439 large geographic extents, and do not suffer the same limitations associated with light
440 availability and cloud coverage as their multispectral counterparts.

441

442 However, active microwave sensors are limited in their ability to penetrate deep soil
443 horizons. Typically, sensors can monitor moisture at a depth equal to about 1/10th to half of
444 the sensor's wavelength. Longer wavelengths result in deeper penetration, with L-band
445 sensors (around 1.4GHz) offering the deepest measurements at around 1-5cm. Microwave
446 sensors tend to have coarse spatial resolution (often kilometres, rather than metres)
447 resulting in studies having a global or continental scale; unlike passive sensors which have
448 much finer spatial resolution allowing analysis to be undertaken at more local scales. This is
449 often due to a trade-off between antenna size (affecting wavelength size and spatial
450 resolution) and orbital geometry (which affects satellite revisit time) (Pan *et al.*, 2017). In

451 comparison to multispectral sensors, the number of microwave sensors in orbit is smaller,
452 as the former usually have a broader range of applications. Nonetheless, global coverage,
453 long-term records and often short revisit times (daily/weekly) make microwave sensor
454 derived soil moisture estimates valuable for drought monitoring and impact assessment
455 over global, continental and regional scales.

456

457 The SMAP (Soil Moisture Active Passive) mission launched in 2015 was well positioned to
458 revolutionise soil moisture remote sensing (Entekhabi *et al.*, 2010). The goal was a product
459 which merged high spatial resolution active radar and coarse-resolution, but highly
460 sensitive, passive radiometer observations (Entekhabi *et al.*, 2010; Das *et al.*, 2014), to
461 produce relatively high spatial (3km, 9km and 36km) and temporal resolution (2-3 days)
462 data products. Early SMAP data was assessed for accuracy and validity and satisfied all
463 standards (Colliander *et al.*, 2017). However, only 9 months into the mission the on-board
464 radar equipment failed and was deemed unrepairable. However, there have been successful
465 attempts to downscale and produce higher spatial resolution datasets using in-situ field
466 observations and available active-passive algorithms (Das *et al.*, 2018; Wei *et al.*, 2019).
467 There have also been attempts to compare and merge available SMAP products with
468 observations from other active microwave sensors such as ASCAT (Advanced
469 SCATterometer) (Kim *et al.*, 2018), SMOS (Al-Yaari *et al.*, 2017) and Sentinel-1 SAR data (Das
470 *et al.*, 2016) with varying results depending on local conditions. Despite the loss of the on-
471 board radar, recent studies suggest SMAP products have potential for large scale
472 agricultural drought monitoring. Eswar *et al.* (2018) compared SMAP estimates of soil
473 moisture with modelled USDM (US Drought Monitor) and SPI data. Results indicated that
474 SMAP data over 13-26 week intervals was able to accurately capture changing drought

475 intensity levels. Bai *et al.* (2018) used SMAP estimates to calculate the Soil Water Deficit
476 Index (SWDI) for mainland China and concluded that SMAP derived SWDI has good overall
477 performance under drought conditions.

478

479 Launched in 2009, SMOS was the first mission to provide global measurements of L-band
480 brightness temperature. Its microwave radiometer allows for remotely sensed estimation of
481 soil moisture (and ocean salinity) with a spatial resolution of approximately 43-50km and a
482 revisit time of less than three days (Kerr *et al.*, 2010). Like SMAP, studies using SMOS soil
483 moisture retrievals suggest that the satellite is well suited to support the monitoring of
484 agricultural drought, through both direct sensor observations or the data product's utility in
485 calculating agricultural drought indices (e.g. Sánchez *et al.*, 2016; Pablos *et al.*, 2017;
486 Tagesson *et al.*, 2018). The SMOS mission is reported to be in excellent technical condition
487 (Mecklenburg *et al.*, 2016), so it is likely that the sensors role in agricultural drought
488 monitoring will continue to grow.

489

490 The AMSR-E (Advanced Microwave Scanning Radiometer - Earth Observing System), also
491 equipped with a passive microwave radiometer, has shown similar potential for effective
492 drought monitoring (e.g. Rao *et al.*, 2019). The AMSR-E observation record is made up of
493 daily 25km (resampled) soil moisture products from 2002-2011. AMSR-E historic products
494 have been reanalysed to calculate various agricultural drought indices and results show that
495 the data record has good potential for the representation of long-term drought events over
496 large spatial scales (Champagne *et al.*, 2011; Abelen *et al.*, 2015; Draper & Reichle, 2015;
497 Zhang *et al.*, 2017a; Liu *et al.*, 2017). As with multispectral sensors, a range of active and
498 passive microwave sensors, including those discussed above, have been evaluated against

499 in-situ measurements with generally positive results, although this is dependent on
500 analytical procedures and local characteristics (Al-Yaari *et al.*, 2019; Zhang *et al.*, 2019).

501

502 **5.0 Integrated Approaches to Drought Monitoring**

503 Zhang *et al.* (2017a) highlight the importance of a multi-/integrated index approach to
504 drought monitoring. Many studies use various remote sensing products to simultaneously
505 explore multiple drought types. Nicolai-Shaw *et al.* (2017) used GLEAM data as an additional
506 factor for agricultural drought monitoring, by exploiting the link between evaporation and
507 vegetation condition. The delay in the response of vegetation to peaks in evapotranspiration
508 was of particular interest; which the authors attribute to a potential limitation of GLEAM
509 data - the underestimation of water availability in deeper soil horizons which supports plant
510 growth. In a similar study, Orth & Destouni (2018) used various remote sensing data
511 products to assess water balance disequilibrium during droughts across mainland Europe. In
512 particular, they focused on the relationship between various hydrological cycle stages, such
513 as precipitation, evapotranspiration (GLEAM), vegetation condition (vegetation index
514 based), and runoff. GLEAM data was incorporated to reveal patterns in evapotranspiration,
515 which lagged significantly behind variations in runoff following drought onset in southern
516 Europe, suggesting that agricultural drought reduces runoff faster than it reduces
517 evapotranspiration.

518

519 Remotely sensed data products have also been used to calculate new integrated monitoring
520 indices designed to monitor various drought types. For example, Du *et al.* (2013) propose
521 the Synthesized Drought Index (SDI) – a principal components product combining the
522 Vegetation Condition Index (VCI) (Kogan 1995a), the Temperature Condition Index (TCI)

523 (Kogan 1995b) and the PCI. The uniqueness of the SDI is the integration of remote sensing
524 data products derived from MODIS and TRMM, allowing an integrated assessment of
525 precipitation deficit, soil moisture depletion and vegetation stress as drought propagates.
526 The integration of indices and different remote sensing derived data products is an
527 important development in effective drought monitoring across multiple drought 'types'.
528 This is highlighted by Zhang *et al.* (2017a) who found that shorter-term dry events are not
529 fully represented in many agricultural or hydrological drought indices; which are better
530 suited for longer-term drought monitoring. Therefore, there is a need to use some form of
531 meteorological index alongside these measures to fully examine drought propagation and
532 short-term meteorological droughts.

533

534 Even when monitoring a small number of drought-related variables it is important to
535 consider a range of comparable datasets from different sensor types (Hao *et al.*, 2015). For
536 agricultural drought monitoring, Zhang *et al.* (2017a) show how different soil moisture
537 datasets and indices are correlated with different length accumulation periods of SPI data
538 (which represent different drought severity levels). Passive microwave remotely sensed
539 data from AMSR-E, in the form of the Soil Moisture Condition Index (SMCI) (Zhang & Jia,
540 2013), correlated well with short-term SPI in regions with low vegetation cover, while
541 multispectral indices, such as the VCI and TCI, were better correlated with 3-month SPI. The
542 use of multiple remotely sensed soil moisture products is clearly valuable in agricultural
543 drought monitoring as different indices and sensors have particular strengths and
544 weaknesses. However, the relationship will be highly dependent on the characteristics of
545 the land surface variables under observation, for example some vegetation parameters may
546 respond more slowly to drought onset than soil moisture at the same location due to

547 resilient vegetation biophysical characteristics. Other local land surface characteristics will
548 also affect this relationship such as terrain and landcover (Zhang *et al.*, 2017a).

549

550 The development of integrated indices combining traditional meteorological datasets and
551 remote sensing approaches has been of interest in drought monitoring research more
552 recently (Liu *et al.*, 2016). The integration of local field measurements, such as those from
553 soil moisture probes, potentially offers a significant improvement over using remotely
554 sensed data alone. Even with recent advances in remote sensing, it is only possible to
555 measure the soil moisture content of the surface material (1-5cm). This is problematic given
556 that crop roots are usually 10-20cm deep, and consequently root zone soil moisture deficits
557 cannot be determined directly. This could be resolved by incorporating in-situ
558 measurements at deeper depths into drought monitoring techniques, alongside satellite
559 observations. The benefit of such approaches is that the spatial and temporal benefits of the
560 remote sensing approaches are retained, while localised data for soil moisture, precipitation
561 and other variables are also incorporated.

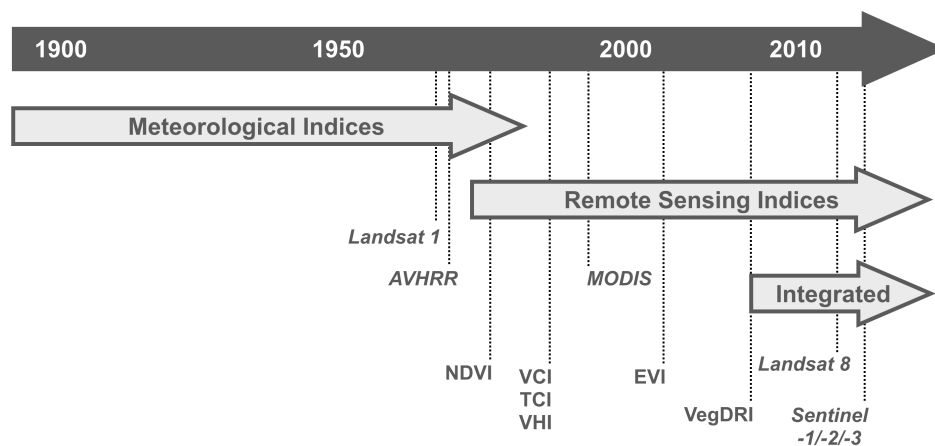
562

563 Brown *et al.* (2008) developed one of the first and most widely applied integrated drought
564 monitoring indices – VegDRI (Vegetation Drought Response Index). VegDRI was developed
565 to exploit the strengths of both remote sensing and climate-based drought monitoring
566 techniques. The remote sensing component provides spatial information about the
567 distribution and general condition of vegetation from NDVI data. VegDRI produces drought-
568 related vegetation stress/condition data at 1km resolution which is updated weekly (Brown
569 *et al.*, 2008). Initially VegDRI was compared against the USDM model and results suggested
570 that VegDRI offered significant advancements. As of 2015, VegDRI features as a part of the

571 new USDM model to enhance the spatial resolution of modelled drought patterns (Hao &
 572 Singh, 2015). Since its development VegDRI has been used in the development of new
 573 models (e.g. Tadesse *et al.*, 2010) and to contribute to drought assessment at a national
 574 scale (e.g. Wu *et al.*, 2013). As new sensors are launched, and datasets developed, it is likely
 575 that remotely sensed data will be incorporated into national scale models and early warning
 576 systems in a similar way (Roy *et al.*, 2014).

577

578 While the benefits of integrating field measurements and traditional meteorological indices
 579 with remote sensing techniques are clear, many studies are still focusing on developing
 580 solely remote sensing-based approaches. Since VegDRI (Brown *et al.*, 2008) was published,
 581 many remote sensing only based techniques have been proposed, such as the Temperature-
 582 Vegetation-Soil Moisture Dryness Index (TVMDI) which utilises LST, soil moisture and NDVI
 583 observations (Amani *et al.*, 2017). This is likely due to newer and more advanced satellites
 584 and sensors having been launched in the interim, such as Sentinel-2 and SMAP. As a result,
 585 recent research has been characterised by the parallel development of both remote sensing
 586 and integrated approaches (Figure 4).



587

588 **Figure 4:** Key milestones and a chronological view of the development of agricultural
 589 drought monitoring indices

590

591 As evidenced previously, a review of the remote sensing literature relating to agricultural
592 drought monitoring found that the NDVI is by far the most commonly applied monitoring
593 method. This is significant given that since its development, many more sophisticated and
594 potentially more representative indices have been developed, including pure remote
595 sensing approaches, and integrative remote sensing and field-based indices. In relation to
596 sensor type, passive sensors/approaches outnumber active in the papers reviewed. This is
597 likely due to a number of factors relating to data availability/resolution/timeliness, ease of
598 application and interpretation, awareness of methods, and what is perceived as 'standard
599 practice' (Bachmair *et al.*, 2016).

600

601 **6.0 Streamflow Monitoring**

602 Agricultural droughts can trigger positive feedback loops in the hydrologic cycle (Teuling *et*
603 *al.*, 2005). Soil moisture will continue to be lost during a drought via evapotranspiration,
604 which will be enhanced due to increased radiation and temperature (Van Loon, 2015). This
605 loss will not be offset with precipitation, reducing the percolation and throughflow of water
606 to recharge groundwater and streamflow (Ivanov *et al.*, 2008). This triggers a hydrological
607 drought, characterised by a deficit in the supply of surface and subsurface water (Sheffield
608 & Wood, 2011). Hydrological drought is often quantified by reduced
609 streamflow/groundwater and low levels in lakes and reservoirs (Tallaksen & Van Lanen,
610 2004). Hydrological droughts occur over long time scales and socio-economic impacts can
611 be severe (Figure 2) (Isaak *et al.*, 2012).

612

613 In comparison with meteorological and agricultural drought, the development of remote
614 sensing-based approaches to hydrological drought has been more limited. In particular,
615 research into the role of remote sensing in providing estimates of river discharge has been
616 minimal due to the lack of sensors/satellites dedicated to this purpose (Lettenmaier *et al.*,
617 2015). Some studies have used basic fluvial geomorphological theory and supplementary in-
618 situ data (river flow gauges) to estimate discharge via remote sensing. Landsat and SAR
619 datasets have been used in this context to provide estimates of channel width to calculate
620 hydraulic geometry relationships (e.g. Smith *et al.*, 1996; Gleason & Smith, 2014; Gleason *et*
621 *al.*, 2014). However, there are no studies to date which apply this within the context of
622 hydrological drought.

623 Through remote sensing technologies it has been possible however to monitor change in
624 Earth's total water storage in association with hydrological/groundwater drought. The
625 Gravity Recovery & Climate Experiment (GRACE) (Tapley *et al.*, 2004) mission launched in
626 2002 was operated by NASA and the German Aerospace Center. The mission originally had a
627 lifespan of 5 years, however due to its successes, the mission was extended until 2017. The
628 GRACE mission consisted of two satellites in tandem orbit. On-board instruments measured
629 the distance between the satellites, which fluctuated at around 200km as a result of Earth's
630 changing gravitational field. These measurements were used to produce monthly
631 representations of changes in the Earth's gravity field. The main drivers being the shifting
632 oceanic/atmospheric/terrestrial distribution of water within the hydrological cycle. GRACE
633 therefore observed terrestrial water storage (TWS) variations in all water storage locations
634 (soil moisture, surface water, and groundwater). GRACE was unique in its non-dependence

635 on surface conditions and being able to provide measurements below the first five
636 centimetres of the surface.

637 GRACE data has been successfully applied in numerous hydrological drought monitoring
638 studies, for example in the analysis of drought event signatures and propagation (Hirschi *et*
639 *al.*, 2006; Yirdsaw *et al.*, 2008; Thomas *et al.*, 2014; Ma *et al.*, 2017), examining regional
640 differences in drought severity (Xavier *et al.*, 2010; Frappart *et al.*, 2013), and monitoring
641 groundwater depletion (Rodell *et al.*, 2009; Zhong *et al.*, 2018). GRACE has also been used
642 to calculate indices which can be applied in large scale hydrological drought monitoring,
643 such as the Drought Severity Index (DSI) (Zhao *et al.*, 2017), the Total Storage Deficit Index
644 (TSDI) (Narasimhan & Srinivasan, 2005; Yirdaw *et al.*, 2008) and the Multivariate
645 Standardised Drought Index (MSDI) (Forootan *et al.*, 2019); most being applied in order to
646 show spatio-temporal changes in drought severity (e.g. Voss *et al.*, 2013; Zhao *et al.*, 2015;
647 Forootan *et al.*, 2016). Recent work has also sought to incorporate GRACE data into complex
648 hydrological and groundwater models (e.g. Schumacher *et al.*, 2018) and in the USDM,
649 GRACE was used to monitor hydrological/groundwater drought.

650 Under drought conditions GRACE data has been used alongside in-situ measurements and
651 other sensors (Forootan *et al.*, 2016), and assessed against climate models (Xia *et al.*, 2016)
652 and established hydrological drought indices. Results suggest that GRACE significantly
653 improved our ability to monitor hydrological/groundwater drought over large spatial and
654 temporal scales (Long *et al.*, 2014; Thomas *et al.*, 2017; Sun *et al.*, 2017). For example,
655 Forootan *et al.* (2019) used GRACE TWS data to assess the global distribution of hydrological
656 drought events and their relationship with atmospheric/oceanic teleconnections. They
657 found that droughts in the Middle East, America and South Asia have increased in intensity

658 in recent years, and that in Asia and Australia hydrological drought events are largely
659 associated with the El Niño Southern Oscillation (Forootan *et al.*, 2019).

660

661 **7.0 Snow Monitoring**

662 Accurate monitoring of snow cover and depth is important for the characterization of
663 hydrological droughts due to snow's role in ensuring constant water supply in many parts of
664 the world (Shaban, 2009; Kumar *et al.*, 2014). A lower than normal winter snowfall could
665 lead to a hydrological drought through reduced streamflow supply later in the water year
666 (AghaKouchak *et al.*, 2015). As with other drought variables, long records and current
667 observations of spatio-temporal consistent snow cover measurements, especially in
668 mountainous upland areas, are not always readily available. Therefore, remote sensing
669 plays an important role in providing these measurements.

670 Multispectral based snow monitoring approaches rely on snow's strong spectral
671 reflectance/signature and discernibility from surrounding landcovers (Pepe *et al.*, 2005;
672 Dozier *et al.*, 2009). Satellites and sensors such as AVHRR, MODIS and ENVISAT have been
673 routinely used in multispectral-based snow cover assessments (Romanov *et al.*, 2000; Pepe
674 *et al.*, 2005) and indices such as the Normalised Difference Snow Index (NDSI) have been
675 proposed (Hall *et al.*, 2002). Validation of multispectral snow cover datasets against in-situ
676 measurements suggests high levels of accuracy, although this is heavily influenced by
677 underlying and neighbouring landcovers (Hall & Riggs, 2007; Simic *et al.*, 2004). A significant
678 limitation however of multispectral snow monitoring is the potential spectral signature
679 confusion between snow cover and clouds, which can lead to notable snow cover
680 overestimation (Wang *et al.*, 2005). Alternatively microwave sensors, which are not limited

681 by cloud cover, can provide estimates of both snow cover and depth (Durand *et al.*, 2008).
682 However, the longer microwave wavelengths, and associated antenna size required to
683 achieve high spatial resolution data (or at least data comparable to that observed by
684 multispectral sensors), has been a technological limitation (Kongoli *et al.*, 2012).

685 In specific relation to drought monitoring, studies have used remotely sensed snow
686 cover/depth estimates in numerous land surface/hydrological models in order to improve
687 streamflow estimates, and therefore monitor hydrological drought events (e.g. Dong *et al.*,
688 2007). Multispectral snow cover estimates have also been used alongside ancillary datasets,
689 such as soil moisture, in more general agricultural and hydrological drought monitoring
690 (Kumar *et al.*, 2012)

691

692 **8.0 Past Challenges & Future Opportunities**

693 The key challenge in the remote sensing of drought in the past has revolved around
694 resolution (spatial, spectral and temporal). Kogan (1997) noted that AVHRR data was used in
695 many of the index development studies that took place at the close of the 20th Century.
696 AVHRR allowed for the development of drought monitoring indices based on a 1-month
697 data publication period. A month, however, could be considered too long a period to assess
698 variation in vegetation condition during a drought, as the water deficit related change in leaf
699 structure occurs between 3 and 7 days (Anyamba & Tucker, 2012). Additionally, weather
700 patterns typically change at an even faster rate which can significantly affect the creeping
701 nature of drought onset and recession (Sen, 2015). Kogan (1997) therefore suggests that
702 one of the key limitations of remote sensing approaches at the time was that the monthly

703 publication interval of data was inadequate. Studies conducted using MODIS and Landsat
704 have also encountered temporal resolution limitations.

705

706 As well as challenges associated with temporal resolution, a recurring limitation of many
707 remote sensing approaches has been the spatial and spectral resolution of sensors. In
708 agricultural drought monitoring, for example, datasets derived using both active and passive
709 sensors have encountered limitations associated with resolution (Becker, 2006; Davies *et*
710 *al.*, 2008; Rao *et al.*, 2019). Often researchers have had to trade-off spatial and spectral
711 resolution when selecting data products (Lavender & Lavender, 2016; West *et al.*, 2018). For
712 example, when using multispectral sensors, it is common for either the spatial resolution
713 not to be high enough to observe low density/dispersed vegetation, or the spectral
714 resolution to be limited in its sensitivity to change in NIR reflection. These technological
715 issues have limited the potential detection of changes in key environmental variables under
716 drought conditions. Davies *et al.* (2016) attempted to use Landsat 8 derived NDVI (at 30m
717 spatial resolution) to assess soil moisture recharge in semi-arid Rajasthan, India. While the
718 results of this study were statistically inconclusive, they add to the body of evidence
719 suggesting a role for remotely sensed NDVI products in providing proxy information for
720 changes in moisture condition when sensors have appropriate spatial and spectral
721 resolutions.

722

723 Following more recent technological advancements and the launch of new satellites/sensors
724 there is renewed potential to address the limitations of previous studies with regard to
725 resolution. The launch of the ESA (European Space Agency) Sentinel-2 multispectral imaging
726 mission has provided a significant improvement in the spatial, spectral and temporal

727 resolution of global coverage freely available multispectral imagery (Drusch *et al.*, 2012).
728 Sentinel-2A was launched in June 2015 and Sentinel-2B in March 2017. From June 2017
729 both satellites have been fully operational giving a revisit time of around 10 days at the
730 equator and 2-3 days towards the poles (with the number of available images for analysis
731 depending on latitude and cloud cover). Each Sentinel-2 satellite is equipped with a single
732 MultiSpectral Instrument (MSI) with a ground-tracked swath of 290km and 13 spectral
733 bands (ranging from 10-60m spatial resolution), including four high spectral resolution
734 bands positioned at the red-edge region of the EMS designed to provide spectrally precise
735 measurements of vegetation condition and leaf chlorophyll content (Gitelson *et al.*, 2005;
736 Delegido *et al.*, 2011; Clevers & Gitelson, 2013; Frampton *et al.*, 2013). Because of its
737 enhanced resolution, initial studies have suggested that the mission has potential for
738 considerable advances in the remote sensing of vegetation (Hill, 2013; Korhonen *et al.* 2017;
739 Sadeghi *et al.*, 2017; Clevers *et al.*, 2017; Lambert *et al.*, 2018; Vanino *et al.*, 2018), which
740 may in turn provide improvements in agricultural drought monitoring.

741

742 West *et al.* (2018) correlated NDVI derived from each NIR band from Sentinel-2 and the
743 standard NIR band from Landsat 8, against ground measured soil moisture in extreme
744 drought conditions and sparse vegetation. While Sentinel-2 NDVI produced significant
745 correlations (variation was found across the different NIR bands and spatial resolution), no
746 significant results were found with NDVI derived from Landsat 8. The spatial dispersion of
747 vegetation may well explain the lack of significant results with Landsat 8 data due to the
748 30m resolution being too coarse to detect the vegetation signal (West *et al.*, 2018). The
749 improved temporal resolution of Sentinel-2 was also noted in this study. As well as NDVI,
750 GPP estimates derived from Sentinel-2 have been explored with promising results

751 (Sakowska *et al.*, 2016). Most research suggests a key role for Sentinel-2 in future drought
752 monitoring. A key research challenge remains however in assessing the relative importance
753 of spatial and spectral resolution in drought monitoring (Dotzler *et al.*, 2015; Lepine *et al.*,
754 2016; Chemura *et al.*, 2017).

755

756 As well as comparative studies, recent research has also sought to combine datasets from
757 Sentinel-2 and Landsat 8. The MSI on-board Sentinel-2 and the OLI (Operational Land
758 Imager) of Landsat 8 have partially overlapping spectral characteristics, and their differing
759 spatial resolutions can be addressed through resampling (e.g. Li *et al.*, 2017). Therefore,
760 there is potential for data from the two to be integrated through data fusion or
761 transformation (e.g. Zhang *et al.*, 2018). Data fusion of Sentinel-2 and Sentinel-3 has also
762 been explored (Korosov & Pozdnyakov, 2016). Given that key drought-related variables such
763 as LST and NDVI can be derived from Sentinel-3's OCLI (Ocean Land and Colour Instrument)
764 and SLSTR (Sea and Land Surface Temperature Radiometer) sensors (Donlon *et al.*, 2012),
765 there may also be significant drought monitoring opportunities using combined Sentinel-2
766 and Sentinel-3 data that have yet to be fully explored (Guzinski & Nieto, 2019).

767

768 Issues around spatial/spectral resolution may also be addressed with the continued rise in
769 number of hyper-spatial/-spectral sensors being launched in the coming years. For example,
770 the planned NASA HypsIRI (Hyperspectral InfraRed Imager), which will be equipped with
771 10nm bands from the visible to short wave infrared segments of the EMS (see Lee *et al.*,
772 2015), should be able to provide valuable measurements for agricultural drought-related
773 monitoring.

774

775 Beyond resolution-related limitations, a key challenge historically has been the shorter-term
776 availability of remotely sensed data for inclusion in drought monitoring practices when
777 compared to traditional in-situ measurements (Liu *et al.*, 2016). For example, the SPI has a
778 conventional requirement of a long-term precipitation record for calculation (Sen, 2015),
779 which until fairly recently has not been available solely from remotely sensed data (e.g. the
780 CHIRPS rainfall dataset). The availability of a long data record is what gives the Landsat
781 series satellites and sensors a particular advantage over newer missions; having a 40-year
782 record comprised of observations from 7 satellites (Roy *et al.*, 2014). With the launch of
783 Landsat 9 (currently scheduled for late 2020) this record will continue to expand allowing
784 new opportunities for long term agricultural drought monitoring practices. The continuation
785 of the Landsat record may also help in tackling limitations associated with Landsat 8's
786 frequency of observation (e.g. West *et al.* 2018). Given the success of the GRACE mission, in
787 hydrological drought monitoring and beyond, the remote sensing community also awaits
788 measurements from the GRACE-FO (Follow On) mission which was successfully launched in
789 May 2018 and will extend the data record of its predecessor.

790

791 As noted above, accurate estimate of river discharge from solely remotely sensed data is
792 still a major ambition (Lettenmaier *et al.*, 2015). The proposed 2020 launch of the ESA SWOT
793 (Surface Water Ocean Topography) mission may well achieve this goal. SWOT is expected to
794 provide estimates of water surface slope, elevation and width for large river systems
795 globally (i.e. those with a minimum width of 100m). Research using synthetic SWOT
796 observations of channel slope and elevation suggest great potential of the mission to
797 reliably estimate river discharge (Andreadis *et al.*, 2007; Biancamaria *et al.*, 2011). While no

798 research has been conducted relating SWOT to hydrological drought monitoring, the above
799 studies suggest the sensor may have potential in this field.

800

801 As well as new sensors, opportunities for effective drought monitoring will continue to
802 expand with new approaches to 'blend' data products, such as the fusion of Landsat,
803 Sentinel-2 and Sentinel-3 discussed above. A key example of a sensor blended data product
804 is the ESA CCI (Climate Change Initiative) SM (Soil Moisture) dataset. The CCI SM dataset
805 combines various active and passive soil moisture datasets into three products: a merged
806 ACTIVE and merged PASSIVE, and a COMBINED active and passive product (Dorigo *et al.*,
807 2017). The current version of the dataset covers the period 1978-2016. The CCI SM dataset
808 has been used in agricultural drought-related research (e.g. Chen *et al.*, 2014; Sawada,
809 2018), with the authors noting the value of the long CCI SM data record. As the data
810 continues to expand temporally and improve in accuracy, it is expected that its utility in the
811 field of drought monitoring will be core to examining long term soil moisture trends. Recent
812 comparisons of CCI SM data and GLDAS (Global Land Data Assimilation) simulated soil
813 moisture show that the two are significantly correlated; showing similar severity and spatial
814 extents of drought events. However, the research concluded that the ESA CCI SM dataset is
815 more effective in drought monitoring, except in highly vegetated areas (Liu *et al.*, 2019);
816 further demonstrating the high potential of this dataset.

817

818 As well as new sensors and data products, new applications of existing datasets and
819 analytical platforms are becoming available as technology continues to advance. For
820 example, recent work has seen SMAP data used to improve estimates of evapotranspiration
821 (Purdy *et al.*, 2018). The utility of the Google EarthEngine in rapidly calculating

822 evaporation/evapotranspiration for meteorological drought monitoring has already been
823 highlighted in this review. The platform allows for analysis of key remote sensing data
824 products, including the full Landsat record from Landsat 4 onwards, Sentinel-2A, MODIS
825 (including VI's, GPP estimates and thermal anomalies), and TRMM and GPM precipitation
826 estimates (Gorelick *et al.*, 2017). However, the platform has still yet to be fully utilised for
827 wider/integrated drought monitoring approaches at a global scale.

828

829 With increased research on the effects of climate change and human activities, the role of
830 anthropogenic influences on drought event propagation and termination is now becoming
831 ever more apparent, suggesting that drought is not only a phenomenon induced by solely
832 natural processes (Van Loon & Van Lanen, 2013; Van Loon *et al.*, 2016). Various methods to
833 assess the role of human activity on drought have been proposed (Rangecroft *et al.*, 2019;
834 Van Loon *et al.*, 2019), however no such research has yet considered the role of remote
835 sensing and earth observation in assessing anthropogenic activity and the association with
836 drought propagation/termination.

837

838 **9.0 Summary**

839 Since, 1970 there has been a fundamental shift in how we approach drought monitoring;
840 moving away from traditional site-based measurements which are often limited in temporal
841 and spatial resolution to the deployment of remote sensing technologies. In 2005 Wilhite &
842 Pulwarty noted four key issues in drought monitoring. These challenges are still relevant
843 today; however we suggest that the application of remote sensing has, and will continue to,
844 help the research community address these:

845

- 846 1. Spatial resolution and coverage: Remote sensing has significantly improved the
847 coverage and spatial resolution of drought-related variables and has allowed for
848 effective water management in data-poor regions (Sheffield *et al.*, 2018). Sensors
849 have large swaths and high temporal resolution, giving frequent global scale
850 coverage. While in the past there have been limitations around spatial resolution
851 (Brown *et al.*, 2008; Davies *et al.*, 2016), as technology advances this will become
852 less of an issue in drought monitoring, particularly as advances are made in the
853 development and deployment of hyper-resolution sensors.
- 854 2. Temporal frequency of observations: Due to the complex nature of drought events,
855 in both their development and termination (Parry *et al.*, 2016), regular observations
856 of key variables are required. Through remote sensing a range of daily to weekly
857 observations are available, such as (sub-)daily rainfall from GPM and weekly/bi-
858 weekly vegetation condition indices from MODIS, Landsat and now Sentinel-2.
859 Frequent observation, in combination with enhanced spatial coverage, of drought-
860 related variables has provided data in what were traditionally data-sparse regions,
861 particularly in the developing world.
- 862 3. A need for a range of drought indicators: There are a large number of remote
863 sensing data products covering almost all phases of drought propagation, the
864 exception being accurate and frequent observations of river discharge. The
865 combined uses of these datasets to calculate drought monitoring indices has allowed
866 for integrated studies monitoring drought propagation to be undertaken at scales
867 previously unavailable to researchers (e.g. Nicolai-Shaw *et al.*, 2017; Orth &
868 Destouni, 2018).

869 4. A lack of understanding of extreme events: Wilhite & Pulwarty (2005) noted this
870 challenge in relation to the monitoring of both floods and droughts. Remote sensing
871 technologies, through the wide range of sensors and data products, have allowed for
872 greater understanding and better-informed decision making across a range of scales.
873 For example, remote sensing is now commonly used to monitor irrigation systems in
874 many very droughty and dry regions, allowing for scarce water resources to be
875 effectively and efficiently managed to support crop growth (e.g. Vanino *et al.*, 2018)

876

877 In the field of drought monitoring the increasing detail, reliability and accuracy of remote
878 sensing data products will enhance our capacity to forecast and monitor all forms of
879 drought and its impacts at a range of spatial and temporal scales. As we move into the
880 future and technology advances, we must extend the use of remote sensing in drought
881 monitoring (Andela *et al.*, 2013). This may be through the launch of new satellites/sensors
882 or developing new approaches and methodologies to reanalyse existing data. We conclude
883 this paper by thanking *Remote Sensing of Environment* for its role as a key platform for
884 dissemination, and the research community for the advances in the field over the last 50
885 years, and now look forward to the continued application of remote sensing for effective,
886 innovative and efficient drought monitoring solutions.

887

888 **Acknowledgements**

889 We would like to thank the three reviewers for their insightful and considered comments
890 and suggestions on this review paper.

891

892 **References**

893 Abelen, S., Seitz, F., Abarca-del-Rio, R. & Güntner, A. 2015. Droughts and floods in the La
894 Plata Basin in soil moisture and GRACE. *Remote Sensing*. Vol.7(6). 7324-7439.
895
896 AghaKouchak, A., Farahmand, A., Melton, F.S., Teixeira, J., Anderson, M.C., Wardlow, B.D. &
897 Hain, C.R. 2015. Remote sensing of drought: Progress, challenges and opportunities,
898 *Reviews of Geophysics*, Vol.53(2), 452-480.
899
900 Ahmadi, B., Ahmadalipour, A., Tootle, G. & Moradkhani, H. 2019. Remote sensing of water
901 use efficient and terrestrial drought recovery across the contiguous United States. *Remote*
902 *Sensing*. Vol.11(6), 731.
903
904 Ahmed, M., Else, B., Eklundh, L., Ardö, J., & Seaquist, J. 2017. Dynamic response of NDVI to
905 soil moisture variations during different hydrological regimes in the Sahel region.
906 *International Journal of Remote Sensing*. Vol.38(19). 5408-5429.
907
908 Al-Yaari, A., Wigneron, J.-P., Dorigo, W., Colliander, A., Pellarin, T., Hahn, S., Mialon, A.,
909 Richaume, P., Fernandez-Moran, R., Fan, L., Kerrm Y,H. & Lannoy, G.De. 2019. Assessment
910 and inter-comparison of recently developed/reprocessed microwave satellite soil moisture
911 products using ISMN ground-based measurements. *Remote Sensing of Environment*.
912 Vol.224, 289-303.
913
914 Allen, R.G., Tasumi, M. & Trezza, R. 2007. Satellite-based energy balance for mapping
915 evapotranspiration with internalized calibration (METRIC) – model. *Journal of Irrigation &*
916 *Drainage Engineering*. Vol.133(4). 380-394

917

918 Alizadeh, M.R. & Nikoo, M.R. 2018. A fusion-based methodology for meteorological drought
919 estimation using remote sensing data. *Remote Sensing of Environment*. Vol.211. 229-247.

920

921 Almazroui, M. 2011. Calibration of TRMM rainfall climatology over Saudi Arabia during
922 1998-2009. *Atmospheric Research*. Vol.99(3-4.), 400-414.

923

924 Al-Yaari, A., Wigneron, J.-P., Kerr, Y., Rodriguez-Fernandez, N., O'Neill, P.E., Jackson, T.J., De
925 Lannoy, G.J.M., Al Bitar, A., Mialon, A., Richaume, P., Walker, J.P., Mahmoodi, A. & Yueh, S.
926 2017. Evaluating soil moisture retrievals from ESA's SMOS and NASA's SMAP brightness
927 temperature datasets. *Remote Sensing of Environment*. Vol.193 257-273.

928

929 Amani, M., Salehi, B., Mahdavi, S., Masjedi, A. & Dehnavi, S. 2017. Temperature-vegetation-
930 soil moisture dryness index (TVMDI). *Remote Sensing of Environment*. Vol.197. 1-14.

931

932 Anav, A., Friedlingstein, P., Beer, C., Ciais, P., Harper, A., Jones, C., Murray-Tortarolo, G.,
933 Papale, D., Parazoo, N.C., Peylin, P., Piao, S., Sitch, S., Viovy, B., Wiltshire, A. & Zhao, M.
934 2015. Spatiotemporal patterns of terrestrial gross primary production: A review. *Reviews of*
935 *Geophysics*. Vol.53(3). 785-818.

936

937 Andela, N., Liu, Y.Y., van Dijk, A.I.J.M., de Jeu, R.A.M. & McVicar, T.R. 2013. Global changes
938 in dryland vegetation dynamics (1988-2008) assessed by satellite remote sensing:
939 Comparing a new passive microwave vegetation density record with reflective greenness
940 data. *Biogeosciences*. Vol.10(10). 6657-6676.

941

942 Andreadis, K.M., Clark, E.A., Lettenmaier, D.P. & Alsdorf, D.E. 2007. Prospects for river
943 discharge and depth estimation through assimilation of swath-altimetry into a raster-based
944 hydrodynamics model. *Geophysical Research Letters*. Vol.34. L10403.

945

946 Anyamba, A. & Tucker, C.J. 2012. Historical perspectives on AVHRR NDVI and vegetation
947 drought monitoring, in Wardlow, B.D., Anderson, M.C. & Verdin, J.P. (eds.). *Remote Sensing
948 of Drought: Innovative Monitoring Approaches*. CRC Press: New York, United States of
949 America. pp. 23-51.

950

951 Assal, T.J., Anderson, P.J. & Sibold, J. 2016. Spatial and temporal trends of drought effects in
952 a heterogeneous semi-arid forest ecosystem. *Forest Ecology & Management*. Vol.365. 137-
953 151.

954

955 Ault, T.R., Mankin, J.S., Cook, B.I., & Smerdon, J.E. 2016. Relative impacts of mitigation
956 temperature and precipitation on 21st Century megadrought in the American Southwest.
957 *Science Advances*. Vol.2(10). e1600873.

958

959 Bachmair, S., Stahl, K., Collins, K., Hannaford, J., Acreman, M., Svoboda, M., Knutson, C.,
960 Smith, K.H., Wall, N, Fuchs, B., Crossman, N.D. & Overton, I.C. 2016. Drought indicators
961 revisited: the need for wider consideration of environment and society. *Wiley
962 Interdisciplinary Reviews: Water*. Vol.3(4).

963

964 Bai, J., Cui, Q., Chen, D., Yu, H., Mao, Z., Meng, L. & Cai, Y. 2018. Assessment of the SMAP-
965 derived Soil Water Deficit Index (SWDI) as an agricultural drought index in China. *Remote*
966 *Sensing*. Vol.10(8). 1302.

967

968 Baker, L.J., Hannaford, J., Chiverton, A. & Svensson, C. 2016. From meteorological to
969 hydrological drought using standardised indicators. *Hydrology and Earth System Science*.
970 Vol.20(6). 3483-2505.

971

972 Baudoin, M.A., Vogel, C., Nortje, K., & Naik, M. 2017. Living with drought in South Africa:
973 Lessons learnt from the recent El Niño drought period. *International Journal of Disaster Risk*
974 *Reduction*. Vol.2., 128-137.

975

976 Bayarjargal, Y., Karnieli, A., Bayasgalan, M., Khudulmir, S., Gandush, C. & Tucker, C.J. 2006. A
977 comparative study of NOAA-AVHRR derived drought indices using change vector analysis.
978 *Remote Sensing of Environment*. Vol.105. 9-22.

979

980 Bayat, B., van der Tol, C. & Verhoef, W. 2018. Integrating satellite optical and thermal
981 infrared observations for improving daily ecosystem functioning estimations during a
982 drought episode. *Remote Sensing of Environment*. Vol.209. 375-394.

983

984 Bayissa, Y., Tadesse, T., Demisse, G. & Shiferaw, A. 2017. Evaluation of satellite-based
985 estimates and application to monitor meteorological drought for the Upper Blue Nile Basin,
986 Ethiopia. *Remote Sensing*. Vol.9(7). 669.

987

988 Becker, M.W. 2006. Potential for satellite remote sensing of groundwater. *Ground Water*.
989 Vol.44(2). 306-318.
990

991 Biancamaria, S., Durand, M., Andreadis, K.M., Bates, P.D., Boone, A., Mognard, M.,
992 Rodríguez, E., Alsdorf, D.E., Lettenmaier, D.P. & Clark, E.A. 2011. Assimilation of virtual wide
993 swath altimetry to improve Arctic river modelling. *Remote Sensing of Environment*.
994 Vol.115(2). 373-381.
995

996 Brown, J.F., Wardlow, B.D., Tadesse, T., Hayes, M.J. & Reed, B.C. 2008. The Vegetation
997 Drought Response Index (VegDRI): A new integrated approach for monitoring drought stress
998 in vegetation. *GIScience & Remote Sensing*. Vol.45(1). 16-46.
999

1000 Calaudio, H.C., Cheng, Y., Fuentes, D.A., Gamon, J.A., Luo, H., Oechel, W., Qui, H.L., Rahman,
1001 A.D. & Sims, D.A. 2006. Monitoring drought effects on vegetation water content and luxes in
1002 chaparral with the 970nm water band index. *Remote Sensing of Environment*. Vol.103(3).
1003 304-311.
1004

1005 Caracciolo, D., Francipane, A., Viola, F., Valerio Noto, L. & Deidda, R. 2018. Performances of
1006 GPM satellite precipitation over the two major Mediterranean islands. *Atmospheric*
1007 *Research*. Vol.213. 309-322.
1008

1009 Cattani, E., Merino, A., Guijarro, J.A. & Levizzani, V. 2018. East Africa rainfall trends and
1010 variability 1983-2015 using three long term satellite products. *Remote Sensing*. Vol.10(6).
1011 931.

1012

1013 Champagne, C., McNairn, H. & Berg, A.A. 2011. Monitoring agricultural soil moisture
1014 extremes in Canada using passive microwave remote sensing. *Remote Sensing of*
1015 *Environment*. Vol.115(10). 2434-2444.

1016

1017 Chao, N., Wang, Z., Jiang, W., & Chao, D. 2016. A quantitative approach for hydrological
1018 drought characterisation in Southwestern China using GRACE. *Hydrogeology Journal*.
1019 Vol.24(4). 892-903.

1020

1021 Chemura, A., Mutanga, O. & Odindi, J. 2017. Empirical modeling of leaf chlorophyll content
1022 in coffee (*Coffea Arabica*) plantations with Sentinel-2 MSI data: Effects of spectral settings,
1023 spatial resolution, and crop canopy cover. *IEEE Journal of Selected Topics in Applied Earth*
1024 *Observations and Remote Sensing*. Vol.10(12). 5541-5550.

1025

1026 Chen, T, De Jeu, R., Liu, Y.Y., Van der Werf, G.R., & Dolman, A.J. 2014. Using satellite based
1027 soil moisture to quantify the water driven variability in NDVI: A case study over mainland
1028 Australia. *Remote Sensing of Environment*. Vol.140. 330-338.

1029

1030 Choi, M., Jacobs, J.M., Anderson, M.C. & Bosch, D.D. 2013. Evaluation of drought indices via
1031 remotely sensed data with hydrological variables. *Journal of Hydrology*. Vol.476. 265-273.

1032

1033 Clevers, J.G.P.W. & Gitelson, A.A. 2013. Remote estimation of crop and grass chlorophyll
1034 and Nitrogen content using red-edge bands on Sentinel-2 and -3. *International Journal of*
1035 *Applied Earth Observation and Geoinformation*. Vol.23,.344-351.

1036

1037 Clevers, J.G.P.W., Kooistra, L. & van den Brande, M.M.M. 2017. Using Sentinel-2 data for
1038 retrieving LAI and leaf and canopy chlorophyll content of a potato crop. *Remote Sensing*.
1039 Vol.9(5). 405.

1040

1041 Coates, A.R., Dennison, P.E., Roberts, D.A. & Roth, K.L. 2015. Monitoring the impacts of
1042 severe drought on Southern California chaparral species using hyperspectral and thermal
1043 infrared imagery. *Remote Sensing*. Vol.7(11). 14276-14291.

1044

1045 Colliander, A., Jackson, T.J., Bindlish, R., Chan, S., Das, N., Kim, S.B., Cosh, M.H., Dunbar, R.S.,
1046 Dang, L., Pashaian, L., Asanuma, J., Aida, K., Berg, A., Rowlandson, T., Bosch, D., Caldwell, T.,
1047 Caylor, K., Goodrich, D., al Jassar, H., Lopez-Baeza, E., Martinez-Fermamdez, J., Gonzalez-
1048 Zamora, A., Livingston, S., McNairn, H., Pacheco, A., Moghaddam, M., Montzka, C.,
1049 Notarnicola, C., Niedrist, G., Pellarin, T., Prueger, J., Pulliainen, J., Rautiainen, K., Ramos, J.,
1050 Seyfried, P., Su, Z., Zeng, Y., van der Velde, R., Thibeault, M., Dorigo, W., Vreugdenhil, M.,
1051 Walker, J.P., Wu, X., Monerris, A., O'Neil, P.E., Entekhabi, D., Njoku, E.G. & Yueh, S. 2017.
1052 Validation of SMAP surface soil moisture products with core validation sites. *Remote*
1053 *Sensing of Environment*. Vol.191. 215-231.

1054

1055 Cook, B.I., Anchukaitis, K.J., Touchan, R., Meko, D.M. & Cook, E.R. 2016. Spatiotemporal
1056 drought variability in the Mediterranean over the last 900 years. *Journal of Geophysical*
1057 *Research*. Vol. 121(5). 2060-2074.

1058

1059 Das, N.N., Entekhabi, D., Dunbar, R.S., Colliander, A., Chen, F., Crow, W., Jackson, T.J., Berg,
1060 A., Bosh, D.D., Caldwell, T., Cosh, M.H., Collins, C.H., Lopez-Baeza, E., Moghaddam, M.,
1061 Rowlandson, T., Starks, P.J., Thibeault, M., Walker, J.P., Wu, X., O'Neill, P.E., Yueh, S. &
1062 Njoku, E.G. 2018. The SMAP mission combined active-passive soil moisture product at 9km
1063 and 3km spatial resolutions. *Remote Sensing of Environment*. Vol.211. 204-217.
1064
1065 Das, N.N., Entekhabi, D., Njoku, E.G., Shi, J.J.C., Johnson, J.T. & Colliander, A. 2014. Tests of
1066 the SMAP combined radar and radiometer algorithm using airborne field campaign
1067 observations and simulated data. *IEEE Transactions on Geoscience and Remote Sensing*.
1068 Vol.52(4). 2018-2028.
1069
1070 Das, N.N., Entekhabi, D., Kim, S., Yueh, S. & O'Neill, P. 2016. Combining SMAP and Sentinel
1071 data for high-resolution soil moisture product. *IEEE International Geoscience and Remote*
1072 *Sensing Symposium (IGARSS)*. Beijing, China. 10-15 July 2016.
1073
1074 Davies, T., Everard, M. & Horswell, M. 2016. Community-based groundwater and ecosystem
1075 restoration in semi-arid North Rajasthan (3): Evidence from remote sensing. *Ecosystem*
1076 *Services*. Vol.21(A). 20-30.
1077
1078 Delegido, J., Verrelst, J., Alonsa, L. & Moreno, J. 2011. Evaluation of Sentinel-2 red-edge
1079 bands for empirical estimation of green LAI and chlorophyll content. *Sensors*. Vol.11(7).
1080 7063-7081.
1081

1082 Dong, J., Walker, J.P., Houser, P.R. & Sun, C. 2007. Scanning multichannel microwave
1083 radiometer snow water equivalent assimilation. *Journal of Geophysical Research*. Vol.112,
1084 D07106.

1085

1086 Dong, J., Xiao, X., Wagle, P., Zhang, G., Zhou, Y., Jin, C., Torn, M.S., Meyers, T.P., Suyker, A.E.,
1087 Wang, J., Yan, H., Biradar, C. & Moore III, B. 2015. Comparison of four EVI-based models for
1088 estimating gross primary production of maize and soybean croplands and tallgrass prairie
1089 under severe drought. *Remote Sensing of Environment*. Vol.162. 154-168.

1090

1091 Donlon, C., Berruit, B., Buongiorno, A., Ferreora, M.-H., Féménias, P., Frerick, J., Goryl, P.,
1092 Klein, U., Laur, H., Mavrocordatos, C., Nieke, J., Rebhan, H., Seitz, B., Stroede, J. & Sciarra, R.
1093 2012. The Global Monitoring for Environment and Security (GMES) Sentinel-3 mission.
1094 *Remote Sensing of Environment*. Vol.120. 37-57.

1095

1096 Dorigo, W., Wagner, W., Albergel, C., Albrecht, F., Balsamo, G., Brocca, L., Chung, D., Ertl,
1097 M., Forkel, M., Gruber, A., Haas, E., Hamer, P.D., Hirschi, M., Ikonen, J., de Jeu, R., Kidd, R.,
1098 Lahoz, W., Liu, Y.Y., Miralles, D., Mistelbauer, T., Nicoli-Shaw, N., Parinussa, R., Pratola, C.,
1099 Reimer, C., van der Schalie, R., Seneviratne, S.I., Smolander, T. & Lecomte, P. 2017. ESA CCI
1100 Soil Moisture for improved earth system understanding: State-of-the art and future
1101 directions. *Remote Sensing of Environment*. Vol.203. 185-215.

1102

1103 Dotzler, S., Hill, J., Buddenbaum, H. & Stoffels, J. 2015. The potential of EnMAP and Sentinel-
1104 2 data for detecting drought stress phenomena in deciduous forest communities. *Remote*
1105 *Sensing*. Vol.7(10). 14227-14258.

1106

1107 Doughty, R., Xiao, X., Wu, X., Zhang, Y., Bajgain, R., Zhou, Y., Qin, Y., Zou, Z., McCarthy, H.,
1108 Friedman, J., Wagle, P., Basara, J., Steiner, J. 2018. Responses of gross primary production of
1109 grasslands and croplands under drought, pluvial, and irrigation conditions during 2010-2016,
1110 Oklahoma, USA. *Agricultural Water Management*. Vol.204. 47-59.

1111

1112 Dozier, J., Green, R.O., Nolin, A.W. & Painter, T.H. 2009. Interpretation of snow properties
1113 from imaging spectrometry. *Remote Sensing of Environment*. Vol.113(1), 25-37.

1114

1115 Draper, C. & Reichle, R. 2015. The impact of near-surface soil moisture assimilation at
1116 subseasonal, seasonal, and inter-annual timescales. *Hydrology & Earth System Science*.
1117 Vol.19. 4831-4844.

1118

1119 Drusch, M., Bello, D., Carlier, S., Colin, O., Fernandez, V., Gascon, F., Hoersch, B., Isola, C.,
1120 Laberinti, P., Martimort, P., Meygret, A., Spoto, F., Sy, O., Marchese, F. & Bargellini, P. 2012.
1121 Sentinel-2: ESA's optical high resolution mission for GMES Operational Services. *Remote*
1122 *Sensing of Environment*. Vol.120, 25-36.

1123

1124 Du, L., Tian, Q., Yu, T., Meng, Q., Jancso, T., Udvardy, P. & Huang, Y. 2013. A comprehensive
1125 drought monitoring method integrating MODIS and TRMM data. *International Journal of*
1126 *Applied Earth Observation and Geoinformation*. Vol.23. 245-253.

1127

1128 Durand, M., Molotch, N.P. & Margulis, S.A. 2008. Merging complementary remote sensing
1129 datasets in the context of snow water equivalent reconstruction. *Remote Sensing of*
1130 *Environment*. Vol.112(3), 1212-1225.

1131

1132 Dutra, E., Wetterhall, F., Giuseppe, F.D., Naumann, G., Barbosa, P., Vogt, J., Pozzi, W. &
1133 Pappenberger, F. 2014. Global meteorological drought – Part 1: Probabilistic monitoring.
1134 *Hydrology & Earth System Sciences*. Vol.18. 2857-2667.

1135

1136 Eastman, R.R. & Fulk, M. 1993. Long sequence time series evaluation using standardised
1137 principal components. *Photogrammetric Engineering & Remote Sensing*. Vol.59(6). 991-996.

1138

1139 Elhang, K.M. & Zhang, W. 2018. Monitoring and assessment of drought focused on its
1140 impact on Sorghum Yield over Sudan by using meteorological drought indices for the period
1141 2001-2011. *Remote Sensing*. Vol.10(8). 1231.

1142

1143 Entekhabi, D., Njoku, E.G., O'Neill, P., Kellogg, K., Crow, W., Edelstein, W., Entin, J.,
1144 Goodman, S., Jackson, T., Johnson, J., Kimball, J., Peipmeier, J., Koster, R., McDonald, K.,
1145 Moghaddam, M., Moran, S., Reichle, R., Shi, J., Spencer, M., Thurman, S., Tsang, L. & Van
1146 Zyl, J. 2010. The Soil Moisture Active Passive (SMAP) mission. *Proceedings of the IEEE*.
1147 Vol.98(5). 704-716.

1148

1149 Eswar, R., Das, N.N., Poulsen, C., Behrangi, A., Swigart, J., Svoboda, M., Entekhabi, D., Yueh,
1150 S., Doorn, B. & Entin, J. 2018. SMAP soil moisture change as an indicator of drought
1151 conditions. *Remote Sensing*. Vol.10(5). 788.

1152

1153 Fisher, J.B., Melton, F., Middleton, E., Hain, C., Anderson, M., Allen, R., McCabe, M.F., Hook,
1154 S., Baldocchi, D., Townsend, P.A., Kilic, A., Tu, K., Miralles, D.D., Perret, J., Lagouarde, J-P.,
1155 Waliser, D., Purdy, A.J., French, A., Schimel, D., Famiglietti, J.S., Stephens, G. & Wood, E.F.
1156 2017. The future of evapotranspiration: Global requirements for ecosystem functioning,
1157 carbon and climate feedbacks, agricultural management, and water resources. *Water*
1158 *Resources Research*. Vol.53(4). 2618-2626.

1159

1160 Forootan, E., Khandu, J., Awange, J., Schumacher, M., Anyah, R., van Dijk, A.I.J.M. & Kusche,
1161 J. 2016. Quantifying the impacts of ENSO and IOD on rain gauge and remotely sensed
1162 precipitation products over Australia. *Remote Sensing of Environment*. Vol.172. 50-66.

1163

1164 Forootan, E., Khaki, M., Schumacher, M., Wulfmeyer, V., Mehrnegar, N., van Dijk, A.I.J.M.,
1165 Brocca, L., Farzaneh, S., Akinluyi, F., Ramillien, G., Shum, C.K., Awange, J. & Mostafaie, A.
1166 2019. Understanding the global hydrological droughts of 2003-2016 and their relationships
1167 with teleconnections. *Science of The Total Environment*. Vol.650(2). 2587-2604.

1168

1169 Frampton, W.J., Dash, J., Watmough, G, & Milton, E.J. 2013. Evaluating the capabilities of
1170 Sentinel-2 for quantitative estimation of biophysical variables in vegetation. *ISPRS Journal of*
1171 *Photogrammetry and Remote Sensing*. Vol.82. 83-92.

1172

1173 Frappart, F., Seoane, L. & Ramillien, G. 2013. Validation of GRACE derived terrestrial water
1174 storage from a regional approach over South America. *Remote Sensing of Environment*.
1175 Vol.137. 69-83.

1176

1177 Funk, C.C. & Brown, M.E. 2006. Intra-seasonal NDVI change projections in semi-arid Africa.
1178 *Remote Sensing of Environment*. Vol.101(2). 249-256.

1179

1180 Galidaki, G., Zianis, D., Gitas, I., Radoglou, K., Karathanassi, V., Tsakiri-Strati, M.,
1181 Woodhouse, I. & Mallinis, G. 2016. Vegetation biomass estimation with remote sensing:
1182 Focus on forest and other wooded land over the Mediterranean ecosystem. *International*
1183 *Journal of Remote Sensing*. Vol.38(7). 1940-1966.

1184

1185 Gao, B. 1996. A Normalised Difference Water Index for remote sensing of vegetation liquid
1186 water from space. *Remote Sensing of Environment*. Vol.58(3). 257-266.

1187

1188 Garrity, S.R., Allen, C.D., Brumby, S.P., Gangodagamage, C., McDowell, G. & Cai, D.M. 2013.
1189 Quantifying tree mortality in a mixed species woodland using multitemporal high spatial
1190 resolution satellite imagery. *Remote Sensing of Environment*. Vol.129. 54-65.

1191

1192 Gatlin, J.A., Sullivan, R.J. & Tucker, C.J. 1984. Considerations of and improvements to large
1193 scale vegetation monitoring. *IEEE Transactions on Geoscience & Remote Sensing*. Vol.22(6).
1194 496-502.

1195

1196 Gilabert, M.A., Moreno, A., Maselli, F., Martínez, B., Chiesi, M., Sánchez-Ruiz, S., García-
1197 Haro, F.J., Pérez-Hoyos, A., Campos-Taberner, M., Pérez-Priego, O., Serrano-Ortiz, P. &
1198 Carrara, A. 2015. Daily GPP estimates in Mediterranean ecosystems by combining remote

1199 sensing and meteorological data. *ISPRS Journal of Photogrammetry and Remote Sensing*.
1200 Vol.102. 184-197.
1201
1202 Gitelson, A.A., Arkebaurer, T.J. & Suyker, A.E. 2018. Convergence of daily light use efficiency
1203 in irrigated and rainfed C3 and C4 crops. *Remote Sensing of Environment*. Vol.217. 30-37.
1204
1205 Gitelson, A.A., Viña, A., Ciganda, V., Rundquist, D.C. & Arkebauer, T.J. 2005. Remote
1206 estimation of canopy chlorophyll content in crops. *Geophysical Research Letters*. Vol.32(8).
1207 L08403.
1208
1209 Gleason, C.J. & Smith, L.C. 2014. Toward global mapping of river discharge using satellite
1210 images and at-many-stations hydraulic geometry. *Proceedings of the National Academy of*
1211 *Sciences of the United States of America*. Vol.111. 4788-4791.
1212
1213 Gleason, C.J., Smith, L.C. & Lee, J. 2014. Retrieval of river discharge solely from satellite
1214 imagery and at-many-stations hydraulic geometry: Sensitivity to river form and optimization
1215 parameters. *Water Resources Research*. Vol.50(2). 9604-9619.
1216
1217 Gorelick, N., Hancher, M., Dixon, M., Ilyushchenko, S., Thau, D. & Moore, R. 2017. Google
1218 Earth Engine: Planetary scale analysis for everyone. *Remote Sensing of Environment*.
1219 Vol.202. 18-27.
1220

1221 Gu, Y. Hunt, E., Wardlow, B., Basra, J.B., Brown, J.F. & Verdin, J.P. 2008. Evaluation of
1222 MODIS NDVI and NDWI for vegetation drought monitoring using Oklahoma Mesonet soil
1223 moisture data. *Geophysical Research Letters*. Vol.35(22). L22401.
1224
1225 Gutman, G.G. 1990. Towards monitoring droughts from space. *Journal of Climate*. Vol.3(2).
1226 282-295.
1227
1228 Gutman, G.G. 1991. Vegetation indices from AVHRR data: An update and future prospects.
1229 *Remote Sensing of Environment*. Vol.35(2-3). 121-136.
1230
1231 Guzinski, R. & Nieto, H. 2019. Evaluating the feasibility of using Sentinel-2 and Sentinel-3
1232 satellites for high resolution evapotranspiration estimations. *Remote Sensing of*
1233 *Environment*. Vol.221, 157-172.
1234
1235 Haboudane, D., Miller, J.R., Pattey, E., Zarco-Tejada, P.J. & Strachan, I.B. 2004. Hyperspectral
1236 vegetation indices and novel algorithms for predicting green LAI of crop canopies: Modelling
1237 and validation in the context of precision agriculture. *Remote Sensing of Environment*.
1238 Vol.90(3). 337-352.
1239
1240 Hall, D.K., Riggs, G.A., Salomonson, V.V., DiGirolamo, N.E. & Bayr, K.J. 2002. MODIS snow
1241 cover-products. *Remote Sensing of Environment*. Vol.83(1), 181-194.
1242
1243 Hall, D.K. & Riggs, G.A. 2007. Accuracy assessment of the MODIS snow-cover products.
1244 *Hydrological Processes*. Vol.21, 1534-1547.

1245

1246 Hao, C., Zhang, J. & Yao, F. 2015. Combination of multi-sensor remote sensing data for
1247 drought monitoring over Southwest China. *International Journal of Applied Earth*
1248 *Observation and Geoinformation*. Vol.35. 270-283.

1249

1250 Hao, Z. & Singh, V.P. 2015. Drought characterization from a multivariate perspective: A
1251 review. *Journal of Hydrology*. Vol.527. 668-678.

1252

1253 Hayes, M.J., Svoboda, M.D., Wardlow, B.D., Anderson, M.C. & Kogan, F. 2012. Drought
1254 Monitoring, in Wardlow, B.D., Anderson, M.C. & Verdin, J.P. (eds). *Remote Sensing of*
1255 *Drought: Innovative Monitoring Approaches*. CRC Press: New York.

1256

1257 Hill, M.J. 2013. Vegetation index suites as indicators of vegetation state in grassland and
1258 savanna: An analysis with simulated Sentinel-2 data for a North American transect. *Remote*
1259 *Sensing of Environment*. Vol.137. 94-111.

1260

1261 Hirschi, M., Seneviratne, S. & Schär, C. 2006. Seasonal variations in terrestrial water storage
1262 for major midlatitude river basins. *Journal of Hydrometeorology*. Vol.7(1). 39-60.

1263

1264 Holben, B.N. 1986. Characteristics of maximum-value composite images from temporal
1265 AVHRR data. *International Journal of Remote Sensing*. Vol.7(11). 1471-1434

1266

1267 Holben, B.N. & Fraser, R.S. 1984. Red and near-infrared sensor response to off-nadir
1268 viewing. *International Journal of Remote Sensing*. Vol.5(1). 145-160.

1269

1270 Hou, A.Y., Kakar, R.K., Neeck, S., Azarbarzin, A.A., Kummerow, C.D., Kojima, M., Oki, R.,

1271 Nakamura, K. & Iguchi, T. 2014. The Global Precipitation Measurement Mission. *Bulletin of*

1272 *the American Meteorological Society*. Vol.95. 701-722.

1273

1274 Huang, M., Piao, S., Sun, Y., Ciais, P., Cheng, L., Mao, J., Poulter, B., Shi, X., Zeng, Z. & Wang,

1275 Y. 2015. Change in terrestrial ecosystem water use efficiency over the last three decades.

1276 *Global Change Biology*. Vol.21(6). 2366-2378.

1277

1278 Huete, A.R. 1988. A soil-adjusted vegetation index (SAVI). *Remote Sensing of Environment*,

1279 Vol.25(3). 295-309.

1280

1281 Huete, A.R., Didan, K., Miura, T., Rodriguez, E.P., Gao, X. & Ferreira, L.G. 2002. Overview of

1282 the radiometric and biophysical performance of the MODIS vegetation indices. *Remote*

1283 *Sensing of Environment*. Vol.83(1-2). 195-213.

1284

1285 Huffman, G.J., Adler, R.F., Arkin, P., Chang, A., Ferraro, R., Gruber, A., Janowiak, J., McNab,

1286 A., Rudolf, B. & Schneider, U. 1997. The global precipitation climatology project (GPCP)

1287 combined precipitation dataset. *Bulletin of the American Meteorological Society*. Vol.78(1).

1288 5-20.

1289

1290 Hwang, T., Gholizadeh, H., Sims, D.A., Novick, K.A., Brzostek, E.R., Phillips, R.P., Roman, D.T.,

1291 Robeson, S.M. & Rahman, A.F. 2017. Capturing species-level drought responses in a

1292 temperate deciduous forest using ratios of photochemical reflectance indices between
1293 sunlit and shaded canopies. *Remote Sensing of Environment*. Vol.199. 350-359.
1294
1295 IPCC 2014. Climate Change 2014: Synthesis Report. Contribution of Working Groups I, II, and
1296 III to the Fifth Assessment Report of the Intergovernmental Panel on Climate Change. IPCC:
1297 Geneva, Switzerland. pp. 151.
1298
1299 Isaak, D.J., Wollrab, S., Horan, D. & Chandler, G. 2012. Climate change effects on stream and
1300 river temperatures across the Northwest US from 1980-2009 and implications for Salmonid
1301 fishes. *Climatic Change*. Vol.113(2). 449-524.
1302
1303 Islam, M.N. & Uyeda, H. 2005. Comparison of TRMM 3B42 products with surface rainfall
1304 over Bangladesh. *IGARSS 2005: Proceedings of IEEE International Geoscience and Remote*
1305 *Sensing Symposium*. Vol.1-8. 4112-4115.
1306
1307 Islam, M.N. & Uyeda, H. 2007. Use of TRMM in determining the climatic characteristics of
1308 rainfall over Bangladesh. *Remote Sensing of Environment*. Vol.108(3). 264-276.
1309
1310 Ivanov, V.Y., Bras, R.L., & Vivoni, E.R. 2008. Vegetation-hydrology dynamics in complex
1311 terrain of semi-arid areas: A mechanistic approach to modelling dynamic feedbacks. *Water*
1312 *Resources Research*. Vol.44(3). W03429.
1313

1314 Jasinski, M.F. 1990. Sensitivity of the normalised difference vegetation index to subpixel
1315 canopy cover, soil albedo, and pixel scale. *Remote Sensing of Environment*. Vol.32(2-3). 169-
1316 187.

1317

1318 Jiao, W., Zhang, L., Chang, Q., Fu, D., Cen, Y. & Tong, Q. 2016. Evaluating and enhanced
1319 Vegetation Condition Index (VCI) based on VIUPD for drought monitoring in the continental
1320 United States. *Remote Sensing*. Vol.8(3). 224.

1321

1322 Joiner, J., Yoshida, Y., Zhang, Y., Duveiller, G., Jung, M., Lyapustin, A., Wang, Y. & Tucker, C.J.
1323 2018. Estimation of terrestrial global gross primary production (GPP) with satellite data-
1324 driven models and eddy covariance flux data. *Remote Sensing*. Vol.10(9). 1346.

1325

1326 Kerr, Y.H., Waldteufel, P., Wigneron, J-P., Delwart, S., Cabot, F., Boutin, J., Escorihuela, M-J.,
1327 Font, J., Reul, N., Gruhier, C., Juglea, S.E., Drinkwater, M.R., Hahne, A., Martin-Neira, M. &
1328 Mecklenburg, S. 2010. The SMOS Mission: New tool for monitoring key elements of the
1329 global water cycle. *Proceedings of the IEEE*. Vol.98(5). 666-687.

1330

1331 Kim, H., Parinussa, R., Konings, A.G., Wagner, W., Cosh, M.H., Lakshmi, V., Zohaib, M. &
1332 Choi, M. 2018. Global-scale assessment and combination of SMAP with ASCAT (active) and
1333 AMSR2 (passive) soil moisture products. *Remote Sensing of Environment*. Vol.204. 260-275.

1334

1335 Kogan, F.N. 1994a. Application of vegetation index and brightness temperature for drought
1336 detections. *Advanced Space Research*. Vol.15(11). 91-100.

1337

1338 Kogan, F.N. 1994b. NOAA plays leadership role in developing satellite technology for
1339 drought watch. *Earth Observation Magazine*. September issue. 18-21.
1340
1341 Kogan, F.N. 1995a. Droughts of the late 1980s in the United States derived from NOAA polar
1342 orbiting satellite data. *Bulletin of the American Meteorological Society*. Vol.76. 655-668.
1343
1344 Kogan, F.N. 1995b. AVHRR data for detection and analysis of vegetation stress.
1345 *Meteorological Satellite Data Users Conference*. Winchester, UK. 155-162.
1346
1347 Kogan, F.N. 1997. Global drought watch from space. *Bulletin of the American Meteorological*
1348 *Society*. Vol.78. 621-636.
1349
1350 Kongoli, C., Romanov, P. & Ferraro, R. 2012. Snow cover monitoring from remote sensing
1351 satellites: Possibilities for drought assessment, in Wardlow, B.D., Anderson, M.C. & Verdin,
1352 J.P. (eds.). *Remote Sensing of Drought: Innovative Monitoring Approaches*. CRC Press: New
1353 York, United States of America. pp. 359-386..
1354
1355 Korhonen, L., Hadi, Packalen, P. & Rautiainen, M. 2017. Comparison of Sentinel-2 and
1356 Landsat-8 in the estimation of boreal forest canopy cover and leaf area index. *Remote*
1357 *Sensing of Environment*. Vol.195. 259-274.
1358
1359 Korosov, A.A & Pozdnyakov, D.V. 2016. Fusion of data from Sentinel-2/MSI and Sentinel-
1360 3/OLCI. *Living Planet Symposium*. Prague, Czech Republic. 9-13 May 2016.
1361

1362 Krofcheck, D.J., Eitel, J.U.H., Vierling, L.A., Schulthess, U., Hilton, T.M., Dettweiler-Robinson,
1363 E., Pendleton, R. & Litvak, M.E. 2014. Detecting mortality induced structural and functional
1364 changes in a piñon-juniper woodland using Landsat and RapidEye time series. *Remote*
1365 *Sensing of Environment*. Vol.151. 102-113.

1366

1367 Kumar, S.V., Peters-Lidard, C.D., Mocko, D., Reichle, R., Liu, Y., Arsenault, K.R., Xia, Y., Ek, M.,
1368 Riggs, G., Livneh, B. & Cosh, M. 2014. Assimilation of remotely sensed soil moisture and
1369 snow depth retrievals for drought estimation. *Journal of Hydrometeorology*. Vol.15(6), 2446-
1370 2469.

1371

1372 Kummerow, C., Barnes, W., Kozu, W., Shiue, J. & Simpson, J. 1998. The Tropical Rainfall
1373 Measuring Mission (TRMM) sensor package, *Journal of Atmospheric and Oceanic*
1374 *Technology*. Vol.15(3). 809-817.

1375

1376 Lambert, M-J., Sibiry Traoré, P.C., Blaes, X., Baret, P. & Defourny, P. 2018. Estimating
1377 smallholder crops production at village level from Sentinel-2 time series in Mali's cotton
1378 belt. *Remote Sensing of Environment*. Vol.216. 647-657.

1379

1380 Laliberte, A.S., Rango, A., Havstad, K.M., Paris, J.F., Beck, R.F., McNeely, R. & Gonzalez, A.L.
1381 2004. Object-oriented image analysis for mapping shrub encroachment from 1937 to 2003
1382 in Southern New Mexico. *Remote Sensing of Environment*. Vol.93(1). 198-210.

1383

1384 Lavender, S. & Lavender, A. 2016. *Practical handbook of remote sensing*. CRC Press: Florida,
1385 United States of America.

1386

1387 Lee, C.M., Cable, M.L., Hook, S.J., Green, R.O., Ustin, S.L., Mandl, D.J. & Middleton, E.M.
1388 2015. An introduction to the NASA Hyperspectral InfraRed Imager (HyspIRI) mission and
1389 preparatory activities. *Remote Sensing of Environment*. Vol.167. 6-19.

1390

1391 Lepine, L.C., Ollinger, S.V., Ouimette, A.P. & Martin, M.E. 2016. Examining spectral
1392 reflectance features related to foliar nitrogen in forests: Implications for broad-scale
1393 nitrogen mapping. *Remote Sensing of Environment*. Vol.173. 174-186.

1394

1395 Lettenmaier, D.P., Alsdorf, D., Dozier, J., Huffman, G.J., Pan, M. & Wood, E.F. 2015. Inroads
1396 of remote sensing into hydrologic science during the WRR era. *Water Resources Research*.
1397 Vol.51(9). 7309-7342.

1398

1399 Li, Z., Zhang, H.K., Roy, D.P., Yan, L., Huang, H. & Li, J. 2017. Landsat 15-m panchromatic-
1400 assisted downscaling (LPAD) of the 30-m reflective wavelength bands to Sentinel-2 20-m
1401 resolution. *Remote Sensing*. Vol.9(7). 755.

1402

1403 Libertinio, A., Sharma, Lakshmi, V. & Claps, P. 2016. A global assessment of the timing of
1404 extreme rainfall from TRMM and GPM for improving hydrologic design. *Environmental*
1405 *Research Letters*. Vol.11. 054003.

1406

1407 Liu, L., Liao, J., Chen, Z., Zhou, G., Su, Y., Xiang, Z., Wang, Z., Liu, X., Li, Y., Yu, J., Xiong, X. &
1408 Shao, H. 2017. The microwave temperature vegetation drought index (MTVDI) based on

1409 AMSR-E brightness temperatures for long term drought assessment across China (2003-
1410 2010). *Remote Sensing of Environment*. Vol.199. 302-320.
1411
1412 Liu, W.T. & Kogan, F.N. 1996. Monitoring regional drought using the Vegetation Condition
1413 Index. *International Journal of Remote Sensing*. Vol.17(14). 2761-2782.
1414
1415 Liu, X., Zhu, X., Pan, Y., Li, S., Liu, Y. & Ma, Y. 2016. Agricultural drought monitoring:
1416 Progress, challenges, and prospects. *Journal of Geographical Sciences*. Vol.26(6), 750-767.
1417
1418 Liu, Y., Liu, Y. & Wang, W. 2019. Inter-comparison of satellite-retrieved and Global Land
1419 Data Assimilation System-simulated soil moisture datasets for global drought analysis.
1420 *Remote Sensing of Environment*. Vol.220, 1-18.
1421
1422 Lloyd-Hughes, B. 2014. The impracticality of a universal drought definition. *Theory of*
1423 *Applied Climatology*. Vol.117(3-4). 607-611.
1424
1425 Long, D., Shen, Y., Sun, A., Hong, Y., Longuevergne, L., Yang, Y., Li, B. & Chen, L. 2014.
1426 Drought and flood monitoring for a large karst plateau in southwest China using extended
1427 GRACE data. *Remote Sensing of Environment*. Vol.155. 145-160.
1428
1429 Loveland, T.R., Merchant, J.W., Brown, J.F. & Ohlen, D.O. 1991. Development of a land cover
1430 characteristics database for the conterminous United States. *Photogrammetric Engineering*
1431 *& Remote Sensing*. Vol.57(11). 1453-1463.
1432

1433 Lu, X. & Zhuang, Q. 2010. Evaluating evapotranspiration and water-use efficiency of
1434 terrestrial ecosystems in the conterminous United States using MODIS and AmeriFlux data.
1435 *Remote Sensing of Environment*. Vol.114(9). 1924-1393.
1436
1437 Ma, S., Wu, Q., Wang, J. & Zhang, S. 2017. Temporal evolution of regional drought detected
1438 from GRACE TWSA and CCI SM in Yunnan Province, China. *Remote Sensing*. Vol.9(11). 1124.
1439
1440 Mänd, P., Hallik, L., Peñuelas, J., Nilson, T., Duce, P., Emmett, B.A., Beier, C., Estiarte, J.,
1441 Kalapos, T., Schmidt, I.K., Kovács-Lang, E., Preto, P., Tietema, A., Westerveld, J.W. & Kull, O.
1442 2010. Responses of the reflectance indices PRI and NDVI to experimental warming and
1443 drought in European shrublands along a north-south climatic gradient. *Remote Sensing of*
1444 *Environment*. Vol.114(3). 626-636.
1445
1446 Martens, B., Miralles, D.G., Lievens, H., van der Schalie, R., de Jeu, R.A.M., Fernández-
1447 Prieto, D., Beck, H.E., Dorigo, W.A. & Verhoest, N.E.C. 2017. GLEAM v3: Satellite-based land
1448 evaporation and root-zone soil moisture. *Geoscientific Model Development*. Vol.10. 1903-
1449 1925.
1450
1451 Martínez-Fernández, J., González-Zamora, A., Sanchez, N., Gumuzzio, A. & Herrero-Jiménez,
1452 C.M. 2016. Satellite soil moisture for agricultural drought monitoring: Assessment of the
1453 SMOS derived soil water deficit index. *Remote Sensing of Environment*. Vol.177. 277-286.
1454

1455 McKee, T.B., Doesken, N.J. & Kleist, J. 1993. The relationship of drought frequency and
1456 duration to time scale. *Preprints Eighth Conference on Applied Climatology*. American
1457 Meteorological Society, Anaheim, California. 17-22 January 1993. 179-184.
1458

1459 Mecklenburg, S., Drusch, M., Kaleschke, L., Rodriguez-Fernandez, N., Reul, N., Kerr, Y., Font,
1460 J., Martin-Neira, M., Oliva, R., Daganzo-Eusebio, E., Grant, J.P., Sabia, R., Macelloni, G.,
1461 Rautiainen, K., Fauste, J., de Rosnay, P., Munoz-Sabater, J., Verhoest, N., Lievens, H.,
1462 Delwart, S., Crapolicchio, R., de la Fuente, A. & Kornberg, M. 2016. ESA's Soil Moisture and
1463 Ocean Salinity Mission: From science to operational applications. *Remote Sensing of*
1464 *Environment*. Vol.180. 3-18.
1465

1466 Miralles, D.G., Holmes, T.R.H., De Jeu, R.A.M., Gash, J.H., Meesters, A.G.C.A. & Dolman, A.J.
1467 2011. Global land-surface evaporation estimated from satellite-based observations.
1468 *Hydrology & Earth System Science*. Vol.15. 453-469.
1469

1470 Miralles, D.G., van den Berg, M.J., Gash, J.H., Parinussa, R.M., de Jeu, R.A.M., Beck, H.E.,
1471 Holmes, T.R.H., Jiménez, C., Verhoest, N.E.C., Dorigo, W.A., Tueling, A.J. & Dolman, A.J.
1472 2014. El Niño-La Niña cycle and recent trends in continental evaporation. *Nature Climate*
1473 *Change*. Vol.4. 122-126.
1474

1475 Mishra, A., Vu, T., Veettil, A.V. & Entekhabi, D. 2017. Drought monitoring with soil moisture
1476 active passive (SMAP) measurements. *Journal of Hydrology*. Vol.552. 620-632.
1477

1478 Monteith, J.L. 1972. Solar radiation and productivity in tropical ecosystems. *Journal of*
1479 *Applied Ecology*. Vol.9(3). 747-766.

1480

1481 Morison, J.I.L. & Moorecroft, M.D. 2006. *Plant Growth & Climate Change*. Blackwell
1482 Publishing Ltd: Oxford.

1483

1484 Mutanga, O., Adam, E. & Cho, M.A. 2012. High density biomass estimation for wetland
1485 vegetation using WorldView-2 imagery and random forest regression algorithm.
1486 *International Journal of Applied Earth Observation and Geoinformation*. Vol.18. 399-406.

1487

1488 Myoung-Jin, U., Kim, Y. & Park, D. 2018. Evaluation and modification of the drought severity
1489 index (DSI) in East Asia. *Remote Sensing of Environment*. Vol.209. 66-76.

1490

1491 Nagarajan, R. 2009. *Drought Assessment*. Springer: Berlin.

1492

1493 Narasimhan, B. & Srinivasan, R. 2005. Development and evaluation of soil moisture deficit
1494 index (SMDI) and evapotranspiration deficit index (ETDI) for agricultural drought
1495 monitoring. *Agricultural and Forest Meteorology*. Vol.133(1-4). 69-88.

1496

1497 Neigh, C.S.R., Tucker, C.J. & Townshend, J.R.G. 2008. North American vegetation dynamics
1498 observed with multi-resolution satellite data. *Remote Sensing of Environment*. Vol.112(4).
1499 1749-1772.

1500

1501 Nicolai-Shaw, N., Zscheischler, J., Hirschi, M., Gudmundsson, L. & Seneviratne, S.I. 2017. A
1502 drought event composite analysis using satellite remote sensing-based soil moisture.
1503 *Remote Sensing of Environment*. Vol.203. 216-225.
1504
1505 Nightingale, J.M., Coops, N.C., Waring, R.H. & Hargrove, W.W. 2007. Comparison of MODIS
1506 gross primary production estimates for forests across the USA with those generated by a
1507 simple process model, 3-PGS. *Remote Sensing of Environment*. Vol.109(4). 500-509.
1508
1509 Orth, R. & Destouni, G. 2018. Drought reduces blue-water fluxes more strongly than green-
1510 water fluxes in Europe. *Nature Communications*. Vol.9(1). 3602.
1511
1512 Pablos, M., Martínez-Fernández, J., Sánchez, N. & González-Zamora, A. 2017. Temporal and
1513 spatial comparison of agricultural drought indices from moderate resolution satellite soil
1514 moisture data over Northwest Spain. *Remote Sensing*. Vol.9(11). 1168.
1515
1516 Pal, J.S., Small, E.E. & Eltahir, E.A.B. 2000. Simulation of regional scale water and energy
1517 budgets: Representation of sub-grid cloud and precipitation processes within Reg CM.
1518 *Journal of Geophysical Research*. Vol.105(D24). 29579-29594.
1519
1520 Palmer, W.C. 1965. Meteorological Drought. *US Weather Bureau Research Paper*. Vol.45. 58.
1521
1522 Pan, M., Yuan, X., Lu, H., Li, X. & Qin, G. 2017. Soil moisture estimation using active and
1523 passive remote sensing techniques, in Hong, Y., Zhang, Y. & Khan, S.I. (eds.). *Hydrologic*

1524 *Remote Sensing: Capacity Building for Sustainability and Resilience*. CRC Press: New York,
1525 United States of America. pp. 37-57.

1526

1527 Park, S., Feddema, J.J. & Egbert, S.L. 2004. Impacts of hydrological soil properties on drought
1528 detection with MODIS thermal data. *Remote Sensing of Environment*. Vol.89(1). 53-52.

1529

1530 Parry, S., Prudhomme, C., Wilby, R.L. & Wood, P.J. 2016. Drought termination: Concept and
1531 Characterisation. *Progress in Physical Geography*. Vol.40(6). 743-767.

1532

1533 Peng, Y., Gitelson, A.A. & Sakamoto, T. 2013 Remote estimation of gross primary
1534 productivity in crops using MODIS 259m data. *Remote Sensing of Environment*. Vol.128.
1535 186-196.

1536

1537 Pepe, M., Brivio, P.A., Rampini, A., Rota Nodari, F.R. & Boschetti, M. 2005. Snow cover
1538 monitoring in Alpine regions using ENVISAT optical data. *International Journal of Remote
1539 Sensing*. Vol.26(21), 4661-4667.

1540

1541 Pervez, M.S., Budde, M. & Rowland, J. 2014. Mapping irrigated areas in Afghanistan over the
1542 past decade using MODIS NDVI. *Remote Sensing of Environment*. Vol.149. 155-165.

1543

1544 Prabhakara, K., Hively, W.D. & McCary, G.W. 2015. Evaluating the relationship between
1545 biomass, percent groundcover and remote sensing indices across six winter cover crop fields
1546 in Maryland, United States. *International Journal of Applied Earth Observation and
1547 Geoinformation*. Vol.39. 88-102.

1548

1549 Purdy, A.J., Fisher, J.B., Goulden, M.L., Colliander, A., Halverson, G., Tu, K. & Famiglietti, J.S.

1550 2018. SMAP soil moisture improves global evapotranspiration. *Remote Sensing of*

1551 *Environment*. Vol.219. 1-14.

1552

1553 Qu, C., Hao, X. & Qu, J.J. 2019. Monitoring extreme agricultural drought over the Horn of

1554 Africa (HOA) using remote sensing measurements. *Remote Sensing*. Vol.11(8), 902.

1555

1556 Rahman, A., Roytman, L., Krakauer, N.Y., Nizmuddin, M. & Goldberg, M. 2009. Use of

1557 vegetation health data for estimation of Aus Rice Field in Bangladesh. *Sensors*. Vol.9(4).

1558 2968-2975.

1559

1560 Rajasekaran, E., Das, N.N., Poulsen, C., Behrangi, A., Swigart, J., Svoboda, M., Entekhabi, D.

1561 Yeh, S., Doorn, B. & Entin, J. 2018. SMAP soil moisture change as an indicator of drought

1562 conditions. *Remote Sensing*. Vol.10(5). 788.

1563

1564 Rangecroft, S., Van Loon, A.F., Maureira, H., Verbist, K. & Hannah, D.M. 2019. An

1565 observation-based method to quantify the human influence on hydrological drought:

1566 upstream-downstream comparison. *Hydrological Sciences Journal*. Vol.64(3), 276-287.

1567

1568 Rao, K., Anderegg, W.R., Sala, A., Martinez-Vilalta, J. & Konings, A.G. 2019. Satellite-based

1569 vegetation optical depth as an indicator of drought-driven tree mortality. *Remote Sensing of*

1570 *Environment*. Vol.227, 125-136.

1571

1572 Rodell, M., Velicogna, I. & Famiglietti, J.S. 2009. Satellite-based estimates of groundwater
1573 depletion in India. *Nature*. Vol.460. 999-1002.
1574

1575 Rojas, O., Vrieling, A. & Rembold, F. 2011. Assessing drought probability for agricultural
1576 areas in Africa with coarse resolution remote sensing imagery. *Remote Sensing of*
1577 *Environment*. Vol.115(2). 343-352.
1578

1579 Romanov, P., Gutman, G. & Csiszar, I. 2000. Automated monitoring of snow cover over
1580 North America with multispectral satellite data. *Journal of Applied Meteorology and*
1581 *Climatology*. Vol.39(11), 1866-1880.
1582

1583 Rossini, M., Cogliati, S., Meroni, M., Migliavacca, M., Galvagno, M., Busetto, L., Cremonese,
1584 E., Julitta, T., Siniscalco, C., Morra di Cella, U. & Colombo, R. 2012. Remote sensing-based
1585 estimation of gross primary production in a subalpine grassland. *Biogeosciences*. Vol.9.
1586 2565-2584.
1587

1588 Roy, D.P., Wudler, M.A., Loveland, T.R., Woodcock, C.E., Allen, R.G., Helder, D., Irons, J.R.,
1589 Johnson, D.M., Kennedy, R., Scambos, T.A., Schaaf, C.B., Schott, J.R., Sheng, Y., Vermote,
1590 E.F., Belward, A.S., Cohen, W.B., Gao, F., Hipple, J.D., Hostert, P., Huntington, J., Justice,
1591 C.O., Kilic, A., Kovalsky, V., Lee, Z.P., Lyburner, L., Masek, J.G., McCorkel, J., Shuai, Y.,
1592 Trezza, R., Vogelmann, J., Wynne, R.H. & Zhu, Z. 2014. Landsat-8: Science and product vision
1593 for terrestrial global change research. *Remote Sensing of Environment*. Vol.145. 154-172.
1594

1595 Sadeghi, M., Babaeian, E., Tuller, M. & Jones, S.B. 2017. The Optical Trapezoid Model: A
1596 novel approach to remote sensing of soil moisture applied to Sentinel-2 and Landsat-8
1597 observations. *Remote Sensing of Environment*. Vol.198. 52-68.
1598

1599 Sahoo, A.K., Sheffield, J., Pam, M. & Wood, E.F. 2015. Evaluation of the Tropical Rainfall
1600 Measuring Mission multi-satellite precipitation analysis (TMPA) for assessment of large scale
1601 meteorological drought. *Remote Sensing of Environment*. Vol.159. 181-193.
1602

1603 San Miguel Ayanz, J., Vogt, J., De Roo, A. & Schmuck, G. 2000. Natural hazards monitoring:
1604 Forest fires, droughts and floods: The example of European pilot projects. *Surveys in*
1605 *Geophysics*. Vol.21(2-3). 291-305.
1606

1607 Sánchez, N., González-Zamora, A., Piles, M. & Martínez-Fernández, J. 2016. A New Soil
1608 Moisture Agricultural Drought Index (SMADI) Integrating MODIS and SMOS Products: A Case
1609 of Study over the Iberian Peninsula. *Remote Sensing*. Vol.8(4). 287.
1610

1611 Sandholt, I., Rasmussen, K. & Andersen, J. 2002. A simple interpretation of the surface
1612 temperature/vegetation index space for assessment of surface moisture stress. *Remote*
1613 *Sensing of Environment*. Vol.79(2). 213-224.
1614

1615 Sakowska, K., Juszczak, R. & Gianelle, D. 2016. Remote sensing of grassland biophysical
1616 parameters in the context of the Sentinel-2 satellite mission. *Journal of Sensors*. Vol.2016.
1617 4612809.
1618

1619 Sawada, Y. 2018. Quantifying drought propagation from soil moisture to vegetation
1620 dynamics using a newly developed ecohydrological land reanalysis. *Remote Sensing*.
1621 Vol.10(8). 1265.
1622
1623 Sayago, S., Ovando, G. & Bocco, M. 2017. Landsat images and crop model for evaluating
1624 water stress of rainfed soybean. *Remote Sensing of Environment*. Vol.198. 30-39.
1625
1626 Sazib, N., Mladenova, I. & Bolten, J. 2018. Leveraging the Google Earth Engine for drought
1627 assessment using global soil moisture data. *Remote Sensing*. Vol.10(8). 1265.
1628
1629 Schumacher, M., Forootan, E., van Dijk, A.I.J.M., Schmied, H.M., Crosbie, R.S., Kusche, J. &
1630 Döll, P. 2018. Improving drought simulations within the Murray-Darling Basin by combining
1631 calibration/assimilation of GRACE data into the WaterGAP Global Hydrology Model. *Remote*
1632 *Sensing of Environment*. Vol.204. 212-228.
1633
1634 Sen, Z. 2015. *Applied drought modelling, predication and mitigation*. Elsevier: Oxford.
1635
1636 Shaban, A. 2009. Indicators and aspects of hydrological drought in Lebanon. *Water*
1637 *Resources Management*. Vol.23, 1875-1891.
1638
1639 Sheffield, J. & Wood, E.F. 2011. *Drought: Past problems and future scenarios*. Earthscan:
1640 London.
1641

1642 Sheffield, J., Wood, E.F., Pan, M., Beck, H., Coccia, G., Serrat-Capdevila, A. & Verbist, K. 2018.
1643 Satellite remote sensing for water resources management: Potential for supporting
1644 sustainable development in data-poor regions. *Water Resources Research*. Vol.52(12), 9724-
1645 9758.

1646

1647 Simic, A., Fernandes, R., Brown, R., Romnov, P. & Park, W. 2004. Validation of VEGETATION,
1648 MODIS and GOES C SSM/I snow-cover products over Canada based in surface snow depth
1649 observations. *Hydrological Processes*. Vol.18(6), 1089-1104.

1650

1651 Sims, D.A., Rahman, A.F., Cordova, V.D., El-Masri, B.Z., Baldocchi, D.D., Bolstad, P.V.,
1652 Flanagan L.B., Goldstein, A.H., Hollinger, D.Y., Misson, L., Monson, R.K., Oechel, W.C.,
1653 Schmid, H.P., Wofsy, S.C. & Xu, L. 2008. A new model of gross primary productivity for North
1654 American ecosystems based solely on the enhanced vegetation index and land surface
1655 temperature from MODIS. *Remote Sensing of Environment*. Vol.112(4). 1633-1646.

1656

1657 Smith, L.C., Isacks, B.L., Bloom, A.L. & Murray, A.B. 1996. Estimation of discharge from three
1658 braided glacial rivers using synthetic aperture radar satellite imagery: Potential application
1659 to ungagged basins. *Water Resources Research*. Vol.32(7). 2021-2034.

1660

1661 Song, C., Dannenberg, M.P. & Hwang, T. 2013. Optical remote sensing of terrestrial
1662 ecosystem primary productivity. *Progress in Physical Geography: Earth and Environment*.
1663 Vol.37(1). 834-854.

1664

1665 Stone, T.A., Schlesinger, P., Houghton, R.A. & Woodwell, G.M. 1994. A map of the
1666 vegetation of South America based on satellite imagery. *Photogrammetric Engineering &*
1667 *Remote Sensing*. Vol.60. 541-551.

1668

1669 Sun, A.Y., Scanlon, B.R., AghaKouchak, A. & Zhang, Z. 2017. Using GRACE satellite gravimetry
1670 for assessing large-scale hydrologic extremes. *Remote Sensing*. Vol.9(12). 1287.

1671

1672 Sur, C., Hur, J., Kim, K., Choi, W. & Choi, M. 2015. An evaluation of satellite-based drought
1673 indices on a regional scale. *International Journal of Remote Sensing*. Vol.36(22). 5593-5612.

1674

1675 Tadesse, T., Wardlow, B.D., Hayes, M.J., Svoboda, M.D. & Brown, J.F. 2010. The Vegetation
1676 Outlook (VegOut): A new method for predicting vegetation seasonal greenness. *GIScience &*
1677 *Remote Sensing*. Vol.47(1). 25-52.

1678

1679 Tagesson, T., Horion, S., Nieto, H., Fornies, V.Z., González, G.M., Bulgin, C.E., Ghent, D. &
1680 Fensholt, R. 2018. Disaggregation of SMOS soil moisture over West Africa using the
1681 Temperature and Vegetation Dryness Index based on SEVIRI land surface parameters.
1682 *Remote Sensing of Environment*. Vol.206. 424-441.

1683

1684 Tallaksen, L.M. & Van Lanen, H.A.J. 2004. *Hydrological drought: Processes and estimation*
1685 *methods for streamflow and groundwater*. Elsevier Science: Netherlands.

1686

1687 Tang, G., Ma, Y., Long, D., Zhong, L. & Hong, Y. 2016. Evaluation of GPM Day-1 IMERG and
1688 TMPA Version-7 legacy products over Mainland China at multiple spatiotemporal scales.
1689 *Journal of Hydrology*. Vol.533. 152-167.
1690
1691 Tapley, B.D., Bettadpur, S., Ries, J.C., Thompson, P.F. & Watkins, M.M. 2004. GRACE
1692 measurements of mass variability in the earth system. *Science*. Vol.305. 503-505.
1693
1694 Teuling, J., Uijlenhoet, R. & Troch, P.A. 2005. On bimodality in warm season soil moisture
1695 observations. *Geophysical Research Letters*. Vol.32(13). 1-4.
1696
1697 Thomas, B.F., Famiglietti, J.S., Landerer, F.W., Wiese, D.N., Molotch, N.P. & Argus, D.F. 2017.
1698 GRACE groundwater drought index: Evaluation of California Central Valley groundwater
1699 drought. *Remote Sensing of Environment*. Vol.198. 384-392.
1700
1701 Thomas, A.C., Reager, J.T., Famiglietti, J.S. & Rodell, M. 2014. A GRACE-based water storage
1702 deficit approach for hydrological drought characterization. *Geophysical Research Letters*.
1703 Vol.41(5). 1537-1545.
1704
1705 Toté, C., Patricio, D., Boogaard, H., van der Wijngaart, R., Tarnavsky, E. & Funk, C. 2015.
1706 Evaluation of satellite rainfall estimates for drought and flood monitoring in Mozambique.
1707 *Remote Sensing*. Vol.7(2). 1758-1776.
1708

1709 Townshend, J.R.G., Goff, T.E. & Tucker, C.J. 1985. Multi-temporal dimensionality of images
1710 of Normalised Difference Vegetation Index at continental scales. *IEEE Transactions on*
1711 *Geoscience & Remote Sensing*. Vol.23. 888-895.
1712

1713 Tucker, C.J. 1979. Red and photographic infrared combinations for monitoring vegetation.
1714 *Remote Sensing of Environment*. Vol.8(2). 127-150.
1715

1716 Tucker, C.J., Vanpraet, C.L., Boerwinkel, E. & Gaston, A. 1983. Satellite remote sensing of
1717 total herbaceous biomass production in the Senegalese Sahel: 1980-1984. *Remote Sensing*
1718 *of Environment*. Vol.17(3). 461-474.
1719

1720 Ummenhofer, C.C., England, M.H., McIntosh, P.C., Meyers, G.A., Pook, M.J., Risbey, J.S.,
1721 Gupta, A.S., & Taschetto, A.S. 2009. What causes Southeast Australia's worst droughts.
1722 *Geophysical Research Letters*. Vol.36(4). 1-5.
1723

1724 van Dijk, A.I.J.M., Schellekens, J., Yebra, M., Beck, H.E., Renzullo, L.J., Weerts, A. & Donchyts,
1725 G. 2018. Global 5km resolution estimates of secondary evaporation including irrigation
1726 through satellite data assimilation. *Hydrology & Earth System Science*. Vol.22. 4959-4980.
1727

1728 Van Loon, A.F. 2015. Hydrological drought explained. *WIREs Water*. Vol.2. 359-392.
1729

1730 Van Loon, A.F. & Laaha, G. 2015. Hydrological drought severity explained by climate and
1731 catchment characteristics. *Journal of Hydrology*. Vol.526. 3-14.
1732

1733 Van Loon, A.F., Gleeson, T., Clark, J., van Dijk, A.I.J.M., Stahl, K., Hannaford, J., Baldassarre,
1734 G.D., Tueling, A.J., Tallaksen, L.M., Uijlenhoet, R., Hannah, D.M., Sheffield, J., Svoboda, M.,
1735 Verbeiren, B., Wagener, T., Rangelcroft, S., Wanders, N. & Van Lanen, H.A.J. 2016. Drought in
1736 the Anthropocene. *Nature Geoscience*. Vol.9, 89-91.

1737

1738 Van Loon, A.F., Rangelcroft, S., Coxon, G, Brena Naranjo, J.A., Van Ogtrop, F. & Van Lanen,
1739 H.A.J. 2019. Using paired catchments to quantify the human influence on hydrological
1740 droughts. *Hydrological & Earth System Sciences*. Vol.23, 1725-1739.

1741

1742 Van Loon, A.F. & Van Lanen, H.A.J. 2013. Making the distinction between water scarcity and
1743 drought using an observation-modelling framework. *Water Resources Research*. Vol.49,
1744 1483-1502.

1745

1746 Vanino, S., Nino, P., De Michele, C., Bolognwai, S.F., D'Urso, G., Di Bene, C., Penelli, B.,
1747 Vuolo, F., Farina, R., Pulighe, G. & Napoli, R. 2018. Capability of Sentinel-2 data for
1748 estimating maximum evapotranspiration and irrigation requirements for tomato crop in
1749 Central Italy. *Remote Sensing of Environment*. Vol.215. 452-470.

1750

1751 Vinukollu, R.K., Wood, E.F., Ferguson, C.R. & Fisher, J.B. 2011. Global estimates of
1752 evapotranspiration for climate studies using multi-sensor remote sensing data: Evaluation of
1753 three process-based approaches. *Remote Sensing of Environment*. Vol.115(3). 801-823.

1754

1755 Voss, K.A., Famiglietti, M., Lo, C., Linage, C., Rodell, M. & Swenson, S.C. 2013. Groundwater
1756 depletion in the Middle East from GRACE with implications for transboundary water

1757 management in the Tigris-Euphrates-Western Iran region. *Water Resources Research*.
1758 Vol.49(2). 904-914.
1759
1760 Wagle, P., Xiao, X., Torn, M.S., Cook, D.R., Matamala, R., Fischer, M.L., Jin, C., Dong, J. &
1761 Birader, C. 2014. Sensitivity of vegetation indices and gross primary production of tallgrass
1762 prairie to severe drought. *Remote Sensing of Environment*. Vol.152. 1-14.
1763
1764 Wang, C., Qi, S., Niu, Z. Wang, J. 2004. Evaluating soil moisture status in China using the
1765 temperature-vegetation dryness index (TVDI). *Canadian Journal of Remote Sensing*.
1766 Vol.30(5). 671-679.
1767
1768 Wang, L., Sharp, M., Brown, R., Derksen, C. & Rivard, B. 2005. Evaluation of spring snow
1769 covered area depletion in the Canadian Arctic from NOAA snow charts, *Remote Sensing of*
1770 *Environment*. Vol.95(4), 453-463.
1771
1772 Wang, W., Esten, M.W., Svoboda, M.D. & Hafeez, M. 2016. Propagation of drought: From
1773 meteorological drought to agricultural and hydrological drought. *Advances in Meteorology*.
1774 Vol.2016. 1-5.
1775
1776 Wang, X., Hongjie, X., Guan, H. & Zhou, X. 2007. Different responses of MODIS-derived NDVI
1777 to root-zone soil moisture in semi-arid and humid regions. *Journal of Hydrology*. Vol.340.
1778 12-24.
1779

1780 West, H., Quinn, N., Horswell, M. & White, P. 2018. Assessing vegetation response to soil
1781 moisture fluctuation under extreme drought using Sentinel-2. *Water*. Vol.10. 838. DOI:
1782 <https://doi.org/10.3390/w10070838>.
1783
1784 Wei, Z., Meng, Y., Zhang, W., Peng, J. & Meng, L. 2019. Downscaling SMAP soil moisture
1785 estimation with gradient boosting decision tree regression over the Tibetan Plateau. *Remote*
1786 *Sensing of Environment*. Vol.225, 30-44.
1787
1788 Winkler, K., Gessner, U. & Hochschild, V. 2017. Identifying droughts affecting agriculture in
1789 Africa based on remote sensing time series between 2000-2016: Rainfall anomalies and
1790 vegetation condition in context of ENSO. *Remote Sensing*. Vol.9(8). 831.
1791
1792 Wilhite, D.A. & Glantz, M.H. 1985. Understanding the drought phenomenon: The role of
1793 definitions. *Water International*. Vol.10(3). 111-120.
1794
1795 Wilhite, D.A. & Pulwarty, R.S. 2005. Drought and water crises: Lessons learned and the road
1796 ahead, in Wilhite, D.A. (eds.). *Drought & Water Crises: Science, Technology and*
1797 *Management Issues*. CRC Press: Florida.
1798
1799 Wu, J., Zhou, L., Liu, M., Zhang, J., Leng, S. & Dia, C.Y. 2013. Establishing and assessing the
1800 Integrated Surface Drought Index (ISDI) for agricultural drought monitoring in Mid-Eastern
1801 China. *International Journal of Applied Earth Observation and Geoinformation*. Vol.23. 387-
1802 410.
1803

1804 Wulder, M.A., Loveland, T.R., Roy, D.P., Crawford, C.J., Masek, J.G., Woodcock, C.E., Allen,
1805 R.G., Anderson, M.C., Belward, A.S., Cohen, W.B., Dwyer, J., Erb, A., Gao, F., Griffiths, P.,
1806 Helder, d., Hermosilla, T., Hipple, J.D., Hostert, P., Highes, J., Huntington, J., Johnson, D.M.,
1807 Kennedy, R., Kilic, A., Li, Z., Lymburner, L., McCorkel, J., Pahlevan, N., Scambos, T.A., Schaaf,
1808 C., Schott, J.R., Sheng, Y., Storey, J., Vermote, E., Vogelmann, J., White, J.C., Wynne, R.H. &
1809 Zhu, Z. 2019. Current status of Landsat program, science and applications. *Remote Sensing*
1810 *of Environment*. Vol.225, 127-147.

1811

1812 Xavier, L., Becker, M., Cazenave, A., Longuervergne, L., Llovel, W. & Rotunno Filho, O.C. 2010.
1813 Interannual variability in water storage over 2003-2008 in the Amazon Basin from GRACE
1814 space gravimetry, in situ river level and precipitation data. *Remote Sensing of Environment*.
1815 Vol.114(8). 1629-1637.

1816

1817 Xia, L., Zhao, F., Mao, K., Yuan, Z., Zuo, Z. & Xu, T. 2018. SPI-based analysis of drought
1818 changes over the past 60 years in China's major crop-growing areas. *Remote Sensing*.
1819 Vol.10(2). 171.

1820

1821 Xia, Z., Huete, A., Restrepo-Coupe, N., Ma, X., Devadas, R. & Caparelli, G. 2016. Spatial
1822 partitioning and temporal evolution of Australia's total water storage under extreme
1823 hydroclimatic impacts. *Remote Sensing of Environment*. Vol.183. 43-52.

1824

1825 Yan, G., Liu, Y. & Chen, X. 2018. Evaluating satellite-based precipitation products in
1826 monitoring drought events in southwest China. *International Journal of Remote Sensing*.
1827 Vol.39(10). 3186-3214.

1828

1829 Yang, Y., Guan, H., Batelaan, O., McVicar, T.R., Long, D., Piao, S., Liang, W., Liu, B., Jin, Z. &

1830 Simmons, C.T. 2016. Contrasting responses of water use efficiency to drought across global

1831 terrestrial ecosystems. *Nature: Scientific Reports*. 6:23284.

1832

1833 Yirdsaw, S.Z., Snelgrove, K.R. & Agboma, C.O. 2008. GRACE satellite observations of

1834 terrestrial moisture changes for drought characterization in the Canadian Prairie. *Journal of*

1835 *Hydrology*. Vol.356(1-2). 84-92.

1836

1837 Yu, F., Price, K.P., Ellis, J. & Shi, P. 2003. Response of seasonal vegetation development to

1838 climatic variations in eastern central Asia. *Remote Sensing of Environment*. Vol.87(1). 42-54.

1839

1840 Zhang, A. & Jia, G. 2013. Monitoring meteorological drought in semiarid regions using multi-

1841 sensor microwave remote sensing data. *Remote Sensing of Environment*. Vol.134. 12-23.

1842

1843 Zhang, H.K., Roy, D.P., Yan, L., Zhongbin, L., Huang, H., Vermote, E., Skakun, S. & Roger, J-C.

1844 2018. Characterization of Sentinel-2A and Landsat-8 top of atmosphere, surface, and nadir

1845 BRDF adjusted reflectance and NDVI differences. *Remote Sensing of Environment*. Vol.215.

1846 482-494.

1847

1848 Zhang, L., Jiao, W., Zhang, H., Huang, C. & Tong, Q. 2017a. Studying drought phenomena in

1849 the Continental United States in 2011 and 2012 using various drought indices. *Remote*

1850 *Sensing of Environment*. Vol.190. 96-106.

1851

1852 Zhang, Q., Middleton, E.M., Margolis, H.A., Drolet, G.G., Barr, A.A. & Black, T.A. 2009. Can a
1853 satellite-derived estimate of the fraction of PAR absorbed by chlorophyll (FAPAR_{chl}) improve
1854 predictions of light-use efficacy and ecosystem photosynthesis for a boreal aspen forest?.
1855 *Remote Sensing of Environment*. Vol.113(4). 880-888.

1856

1857 Zhang, X., Chen, N., Li, J., Chen, Z. & Niyogi, D. 2017b. Multi-sensor integrated framework
1858 and index for agricultural drought monitoring. *Remote Sensing of Environment*. Vol.188.
1859 141-163.

1860

1861 Zhang, X., Moran, M.S., Zhao, X.Liu, S., Zhou, T., Ponce-Campos, G.E. & Liu, F. 2014. Impact
1862 of prolonged drought on rainfall use efficiency using MODIS data across China in the early
1863 21st Century. *Remote Sensing of Environment*. Vol.150. 188-197.

1864

1865 Zhang, R., Kim, S. & Sharma, A. 2019. A comprehensive validation of the SMAP Enhanced
1866 Level-3 Soil Moisture product using ground measurements over varied climates and
1867 landscapes. *Remote Sensing of Environment*. Vol.223, 82-94.

1868

1869 Zhao, M., Velicogna, I. & Kimball, J.S. 2017. A global gridded dataset of GRACE drought
1870 severity index for 2002-2014: Comparison with PDSI and SPEI and a case study of the
1871 Australia millennium drought. *Journal of Hydrometeorology*. Vol.18(8). 2117-2129.

1872

1873 Zhao, Q., Chen, Q., Jiao, M., Wu, P., Gao, X., Ma, M. & Hong, Y. 2018. The temporal-spatial
1874 characteristics of drought in the Loess Plateau using the remote-sensed TRMM precipitation
1875 data from 1998 to 2014. *Remote Sensing*. Vol.10(6). 838.

1876

1877 Zhao., Q., Wu, W. & Wu, Y. 2015. Variations in China's terrestrial water storage over the
1878 past decade using GRACE data. *Geodesy and Geodynamic*. Vol.6(3). 187-193.

1879

1880 Zhong, Y., Zhang, M., Feng, W., Zhang, Z., Shen, Y. & Wu, D. 2018. Groundwater depletion in
1881 the West Liaohe River Basin, China and its implications revealed by GRACE and in situ
1882 measurements. *Remote Sensing*. Vol.10(4). 493.

1883

1884 Zribi, M., Dribi, G., Amri, R. & Lili-Chananne, Z. 2016. Analysis of the effects of drought on
1885 vegetation cover in a Mediterranean region through the use of SPOT-VGT and TERRA-
1886 MODIS long time series. *Remote Sensing*. Vol.8(12). 992.

1887

1888 **Figure Captions**

1889 **Figure 1:** Number of papers relating to drought (in both paper titles and keywords) in
1890 *Remote Sensing of Environment* and *Web of Science* since 1982. Search terms included
1891 various versions of 'Drought' and 'Remote Sensing'.

1892

1893 **Figure 2:** Different types of drought, their interactions and associated impacts (Adapted
1894 from Van Loon, 2015)

1895

1896 **Figure 3:** Treemap of monitoring approaches used in agricultural drought monitoring of the
1897 papers reviewed. Papers were sourced from a range of journals including *Remote Sensing of*
1898 *Environment, Remote Sensing, and the International Journal of Remote Sensing*.

1899

1900 **Figure 4:** Key milestones and a chronological view of the development of agricultural
1901 drought monitoring indices